

INFORMATION TO USERS

This reproduction was made from a copy of a document sent to us for microfilming. While the most advanced technology has been used to photograph and reproduce this document, the quality of the reproduction is heavily dependent upon the quality of the material submitted.

The following explanation of techniques is provided to help clarify markings or notations which may appear on this reproduction.

1. The sign or "target" for pages apparently lacking from the document photographed is "Missing Page(s)". If it was possible to obtain the missing page(s) or section, they are spliced into the film along with adjacent pages. This may have necessitated cutting through an image and duplicating adjacent pages to assure complete continuity.
2. When an image on the film is obliterated with a round black mark, it is an indication of either blurred copy because of movement during exposure, duplicate copy, or copyrighted materials that should not have been filmed. For blurred pages, a good image of the page can be found in the adjacent frame. If copyrighted materials were deleted, a target note will appear listing the pages in the adjacent frame.
3. When a map, drawing or chart, etc., is part of the material being photographed, a definite method of "sectioning" the material has been followed. It is customary to begin filming at the upper left hand corner of a large sheet and to continue from left to right in equal sections with small overlaps. If necessary, sectioning is continued again--beginning below the first row and continuing on until complete.
4. For illustrations that cannot be satisfactorily reproduced by xerographic means, photographic prints can be purchased at additional cost and inserted into your xerographic copy. These prints are available upon request from the Dissertations Customer Services Department.
5. Some pages in any document may have indistinct print. In all cases the best available copy has been filmed.

**University
Microfilms
International**

300 N. Zeeb Road
Ann Arbor, MI 48106

8508722

Mukherji, Syamananda

STUDY OF SOME PROPERTIES OF TRANS 1,4 POLYISOPRENE CRYSTALS

City University of New York

PH.D. 1985

University
Microfilms
International 300 N. Zeeb Road, Ann Arbor, MI 48106

STUDY OF SOME PROPERTIES OF TRANS 1,4 POLYISOPRENE CRYSTALS

by

Syamananda Mukherji

A Dissertation submitted to the Graduate Faculty in
Chemistry in partial fulfillment of the requirements
for the degree of Doctor of Philosophy, The City
University of New York

1985

This manuscript has been read and accepted for the Graduate Faculty in Chemistry in satisfaction of the dissertation requirement for degree of Doctor of Philosophy

10/18/84

date

Arthur E. Woodward

Chairman of Examining Committee

10/22/84

date

A. M. [Signature]

Executive Officer

David C. Locke

George Odian

Supervisory Committee

THE CITY UNIVERSITY OF NEW YORK

ABSTRACT

STUDY OF SOME PROPERTIES OF TRANS-1,4-POLYISOPRENE CRYSTALS

by

Syamananda Mukherji

Advisor: Professor Arthur E. Woodward

Stirrer crystallization of a trans-1,4-polyisoprene fraction ($\bar{M}_n = 3 \times 10^5$) was carried out from n-butyl acetate and from n-heptane solutions (2% w/v). Fibrous crystals in the β -form were obtained at temperatures of 46-48°C and 36° to 40°C in the two solvents respectively. At 36° to 46°C from n-butyl acetate and 25°-35°C from n-heptane lamellar crystallization took place leading predominantly to the α form. Melting endotherms and densities for various samples were obtained. The maximum T_{ENDO} for α was 74°C and for β 79°C and the maximum weight fraction crystallinity for β was 0.78. The stability of preformed α nuclei in n-butyl acetate and n-heptane using a fraction with $\bar{M}_n = 2.5 \times 10^5$ was monitored as a function of temperature. The dissolution temperature of fibrous β -TPI with the maximum T_{ENDO} was measured in thirteen liquids and the results analyzed in terms of the Flory-Huggins parameter. The heat of fusion for the α and β form obtained by extrapolation of heat of fusion vs the change in specific volume, were found to be 8.0 and 10 kJ mole⁻¹, respectively. A β to α transformation was found to occur in the presence of n-butyl acetate, heptane and amyl acetate as diluents. From experimental results 74°C is chosen as the temperature at which the α and β forms coexist in the bulk. The pressure coefficients of the melting temperature were

calculated to be 38 and 43°K kilobar⁻¹ and the fold surface free energies recalculated to be 42±1 and 53±1 ergs cm⁻² for the α and β forms, respectively. The number of monomer units per average non-crystalline chain traverse for the most crystalline fibrous β-TPI was estimated at 36. The entropy of fusion of α and β-TPI were calculated to be 30 and 22 JK⁻¹ mole⁻¹, respectively. The contribution to the entropy of fusion made by the volume change on fusion were calculated to be 21 and 18 J/K mole⁻¹ for α and β-TPI, respectively.

ACKNOWLEDGEMENT

I wish to express my deepest gratitude and sincere appreciation to my research mentor, Professor Arthur E. Woodward for his valuable time and excellent guidance and unfailing dedication to the progress of the research project. I would like to extend my thanks to both Professor George Odian and Professor David C. Locke for their most helpful suggestions and discussions.

I am also very grateful to my parents, for their encouragement, and to my wife Sharine, for her help, understanding and patience.

TABLE OF CONTENTS

	Page
ACKNOWLEDGEMENT	v
TABLE OF CONTENTS	vi
List of Figures	viii
List of Tables	x
INTRODUCTION	1
STATEMENT OF THE PROBLEM	22
EXPERIMENTAL	23
1. Samples	23
2. Fractionation	23
3. Crystallization	25
4. Density Measurements	26
5. Dissolution Temperature Measurements	26
6. Differential Scanning Calorimetry	27
7. Wide-Angle X-Ray Diffraction	27
RESULTS	28
1. Stirrer Crystallization of Trans 1,4-Polyisoprene	28
2. Seeded Crystallization of TPI from n-Butyl Acetate an n-Heptane Solutions	33
3. Measurement of Heat of Fusion of TPI Crystals Using DSC..	34
4. Effect of Diluents on the Conversion of β to α Form	40
5. Measurement of Dissoluton Temperature of Stirrer Crystallized β -TPI in Various Solvents and Calculation of Equilibrium Dissolution Temperature	49
6. Crystallization of TPI from the Melt	51

Table of Content Continued

	Page
7. Calculation of the Pressure Coefficient of Melting of α and β -TPI	53
8. Recalculation of the Surface Free Energies of α and β -TPI	56
9. Estimation of Average Length of a Non-Crystalline Chain Traverse in the Fibrous β -TPI	55
10. Calculation of the Entropy of Fusion of α - and β -TPI ...	57
11. X-Ray Diffraction Measurements of α - and β -TPI	58
DISCUSSION	60
CONCLUSIONS	78
SUGGESTIONS FOR FUTURE WORK	79
REFERENCES	81

LIST OF FIGURES

Figure No.	Page
1. Three models for lamellar crystals (a) regular, adjacent reentry (b) Irregular adjacent reentry and (c) non-adjacent reentry	6
2. Schematic representation of a micro shish-kebab indicating the intimate connection of the platelets to the central core	9
3. Gel permeation chromatograms for balata and synthetic trans-1,4-polyisoprene	24
4. Differential scanning calorimetry for stirrer-crystallized trans-1,4-polyisoprene at various crystallization temperatures in heptane and n-butylacetate	29
5. Melting endotherm and density -vs. crystallization temperature for stirrer-crystallized trans-1,4-polyisoprene from n-butyl acetate	30
6. Same as in Fig. 5 but from n-heptane	31
7. Effect of variation of T_R on T_m of seeded crystals grown from n-butyl acetate solution	36
8. Same as in Figure 7 but from n-heptane solution	37
9. DSC scans of seeded crystals of TPI (high molecular weight) in n-butyl acetate, at $T_R =$ (a) 42, (b) 44, (c) 46, (d) 48, (e) 49 and (f) 55°C	38
10. Heat of fusion for α and β trans-1,4-polyisoprene vs. specific volume difference between the sample and a 100% crystalline sample	39

Figure Continued

Figure No.	Page
11. Some examples of heat of fusion curves for TPI samples.....	41
12. DSC scans for (a) synthetic TPI and (b) synthetic TPI swollen for 1 day at 25°C in n-butyl acetate and dried	47
13. DSC scans for synthetic TPI cooled slowly (average rate 7°C/h) from (a) 70, (b) 71, (c) 72, (d) 73, (e) 74, and (f) 75°C	52
14. Lamellar thickness vs. melting temperature for α and β -TPI ..	56
15. "Crystallization Scale" showing the temperatures at which various types of crystallization, morphology and poly- morphic modifications can occur from n-butyl acetate solutions of TPI.....	63

LIST OF TABLES

Table No.	Caption	Page
I.	Polymorphism of Some Flexible Linear Polymers	1
II.	Pressure Coefficient of Melting, Heat of Fusion, Volume Change on Fusion and Equilibrium Melting Point Datas of Some Polymers	17
III.	Comparison of the Calculated and Literature Equilibrium Melting Point	19
IV.	Stirrer Crystallization of Trans-1,4-Polyisoprene	32
V.	Crystallinities (W_c) for Stirrer Crystallized β -Trans-1,4- Polyisoprene	33
VI.	Effect of Redissolution Temperature on α -TPI Nuclei	35
VII.	Preparation condition, Polymorphic Modification, Density (at 25°C), Crystalline Fraction (W_c) and Heat of Fusion of α -and β -TPI Samples	42
VIII.	Effect of Diluents on the DSC Endotherm for TPI	48
IX.	Dissolution Temperature for Trans-1,4-Polyisoprene	49
X.	Values of χ and T_D^* for β -TPI Calculated from $T_n(\text{Exp})$	51
XI.	Values of ΔH_f° and T_m^* for α and β -TPI	53
XII.	Melting Points, T_m , and Lamellar Lengths, L , of Melt-Grown TPI (purified Gutta Percha, $\bar{M}_n = 3.85 \times 10^5$) at Various Crystallization Temperatures	54
XIII.	X-Ray Diffraction Measurements of α -and β -TPI - Interplanar Spacings and Relative Intensities	59
XIV.	Thermodynamic Parameters Characterizing the Fusion of Flexible Linear Polymer	72

INTRODUCTION

Trans-1, 4-polyisoprene, TPI, has two crystal forms, monoclinic, α ,^{1,2} and orthorhombic, β .^{1,3} Conditions have been established⁴⁻¹⁵ for the formation of each of the polymorphic modification from melt and solution and so the properties studied can be properly attributed. The property of a given substance to have more than one characteristic crystalline structure goes under the name of "polymorphism".

Until a few years ago, macromolecular polymorphism had been studied only occasionally and was considered relatively uncommon; however it now appears to be a widespread phenomenon. Among the first cases of macromolecular polymorphism to be observed is that described for TPI.⁴⁻⁶

Table I lists some polymers for which polymorphism has been clearly observed. The polymers without possibility of stereoisomerism are quoted on the left. On the right, the stereoregular polymers are listed: the first two being transtactic, the following four isotactic, the last one being syndiotactic.

TABLE I. Polymorphism of some flexible linear polymers

Devoid of Stereoisomerism	Stereoregular
Polyethylene	Transtactic polyisoprene
Polytetrafluoroethylene	Transtactic polybutadiene
Polyoxymethylene	Isotactic polypropylene
Polyvinylidene fluoride	Isotactic polybutene-1
Nylon 6	Isotactic polypentene-1
Nylon 8	Isotactic polyheptene-1
Other polyamides	Syndiotactic polypropylene

The melting of the equilibrium crystals of a polymer is a first order phase transition, so at the melting point T_m^* the following relation holds:

$$T_m^* = \frac{\Delta H_f^0}{\Delta S_f^0} \quad (1)$$

Where ΔH_f^0 is the heat of fusion per mole of the repeating structural units of the polymer chain and ΔS_f^0 is the corresponding entropy of fusion.

The stability of the polymorphs can be discussed in terms of their respective free energies of fusion per repeating unit. At temperatures not too far removed from T_m^* , the free energy of fusion ΔG_f^0 can be written as

$$\Delta G_f^0 = \Delta H_f^0 [1 - (T_m / T_m^*)] \quad (2)$$

If we take the completely liquid polymer as a standard state, the crystalline modification at a given temperature having the greater free energy of fusion per repeating unit should be the more stable one.^{8,11} At a critical temperature, T_m^C , where two crystalline modifications A and B, of a polymer are in equilibrium state, equation (2) can be written as

$$\begin{aligned} \Delta H_f^0 (A) [1 - (T_m^C / T_m^* (A))] \\ = \Delta H_f^0 (B) [1 - (T_m^C / T_m^* (B))] \end{aligned} \quad (3)$$

Now the following cases may arise:

$$(i) \Delta H_f^0 (A) > \Delta H_f^0 (B) \text{ and } T_m^* (A) \geq T_m^* (B)$$

In this case the modification B is a permanently metastable state relative to A and if there is a conversion from B to A occurring, it will be monotropic in character. One example of a monotropic polymeric system is the isotactic polybutene-1¹⁶ system.

$$(ii) \Delta H_f^0 (A) > \Delta H_f^0 (B) \text{ but } T_m^* (A) < T_m^* (B)$$

In this case, we can find a temperature, T_m^C , where there will be a first order phase transition from solid A to solid B and the transition will be enantiotropic. Here the phase A is the low temperature crystal form and the phase B is the high temperature crystal form. The high temperature phase B, has density and ΔS_f^0 , lower than the low temperature phase, A.

Few first-order solid - solid transitions have been established for polymer crystals, possibly because of the sluggishness of equilibration, were it to occur. Since the different solid phases of a polymorphic crystalline polymer can differ substantially in physical properties, specially specific volume, such slow approach to the phase stable at use temperature can cause serious problems in practical applications

as well as in research and quality control. The best known ¹⁶ solid-to-solid phase transitions of crystalline polymers to date are polytetrafluoroethylene, trans-1, 4 - polybutadiene, isotactic polybutene -1, and isotactic polypropylene.

$$(iii) \Delta H_f^0 (A) = \Delta H_f^0 (B) \text{ but } T_m^* (A) > T_m^* (B)$$

This will be the same as case (i).

The melting point of a low molecular weight solid A is lowered by the introduction of a diluent soluble in the melt according to the formula

$$\frac{1}{T_m} - \frac{1}{T_m^*} = - \frac{R}{\Delta H_f} \ln a_A \quad (4)$$

where T_m^* is the melting point of the pure solid A, T_m is the melting point in the presence of a diluent, ΔH_f is the heat of fusion, R the gas constant, and a_A is the activity of A in the melt in the presence of the diluent.

Correspondingly the melting point of the equilibrium crystals of a polymer is depressed by the introduction of a diluent according to the formula ¹⁷ analogous to equation (4).

$$\frac{1}{T_m} - \frac{1}{T_m^*} = \frac{R}{\Delta H_f^0} \frac{1}{x} (\phi - \chi \phi^2) \quad (5)$$

where x is the ratio of the molar volume of the solvent to that of the repeating unit of the polymer, χ is the Flory-Huggin's interaction parameter, and ϕ is the volume fraction of the solvent.

For very dilute solutions, it can be shown that equation (5) becomes¹⁸

$$\frac{1}{T_D^*} - \frac{1}{T_m^*} = \frac{R}{\Delta H_f^0} \cdot \frac{1}{x} \cdot (1 - \chi) \quad (6)$$

where T_D^* is the equilibrium dissolution temperature of the polymer.

Of the thermodynamic parameters, the equilibrium melting point, the heat of fusion, and the equilibrium dissolution temperatures are of fundamental importance in the formal treatment of crystallization and polymorphism in macromolecular systems.

Crystallization of a linear flexible polymer from the melt or solution is restricted by the chain-folding principle.¹⁹⁻²²

Single folded-chain lamellae are usually formed when crystallization of a polymer is carried out isothermally and from dilute solution. TPI was one of the first polymers to be crystallized in the form of single crystals as large as 0.35 mm grown from dilute solution.²³

Measurement of properties conventionally used to determine the crystallinity indicate a notable crystallinity deficiency in polymer single crystals, which in the conventional manner can be interpreted as an amorphous component.

There is a general consensus of opinion that most of the crystalline deficit in dilute solution grown crystals is located along the fold surface. One of the controversial topics in the polymer crystallization field is the nature of the fold surface, particularly whether or not it is reentrant.²³⁻²⁹ Fig. 1 shows three proposed models for the lamellar polymer crystals: (a) shows adjacent re-entry with sharp, regular folding and a uniform fold period; (b) shows adjacent

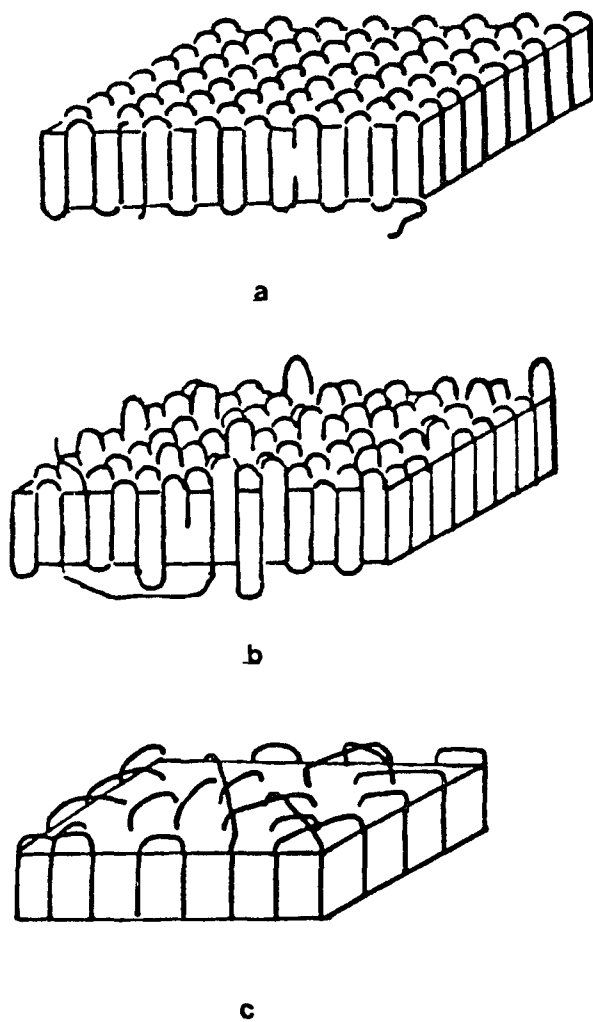


Fig. 1: Three models for the lamellar crystals (a) regular, adjacent reentry (b) Irregular adjacent reentry and (c) non-adjacent reentry.

re-entry with an irregular fold period; and in (c), non adjacent re-entry (switch board model) in which the molecules meander through an amorphous surface layer on the lamella before reentering the lamella or neighboring lamella.

A common but not the sole morphological entity obtained when crystallization is carried out from the melt, is the spherulite. The spherulite consists of stacks of twisted lamellae that emanate radially outward from the center. Noncrystalline portions of the chain in the spherulite can be in the form of crystal defects, chain folds, chain ends and parts of chains which are involved in more than one crystalline lamellar structure. The latter are tie molecules providing much of the cohesion to the structure elements in bulk.

The apparent melting point, (T_m), of a crystalline polymer depends on the crystallization temperature, T_c . As the crystallization temperature increases, thicker lamellas are formed, resulting in a higher melting point. When the lamellar thickness, L , exceeds 200 nm, then the excess surface free energy, σ_e , present in the interfacial area of the polymer crystals does not have much of an effect in lowering the melting point; such crystals can be considered as an equilibrium type but are very difficult to make.

It can be shown³⁰⁻³² from thermodynamic considerations that:

$$T_m = T_m^* (1 - 2 \sigma_e / \Delta H_f^0 L) \quad (7)$$

where σ_e is the end surface free energy and ΔH_f^0 is the heat of fusion per mole of repeat unit. This equation predicts a linear relationship between T_m and $1/L$. σ_e for polyethylene crystals

has been reported¹² to be around 70 ergs. cm⁻². σ_e for α and β - TPI has been calculated⁴⁸ to be 60 and 45 ergs/cm², respectively using experimentally determined L values at various T_m . However, the values of ΔH_f^0 and T_m^* for α and β - TPI used in these calculations are believed to be incorrect.

Recently a number of polymers have been crystallized from solution^{11, 33-43} by the stirrer crystallization technique³³ at high temperatures where ordinary methods of solution crystallization fail. Evidence has been presented to show that a larger crystalline thickness is associated with increasing crystallization temperature and so the stirrer grown crystals of a linear and sufficiently flexible macromolecule, at high crystallization temperature, are expected to be close to the equilibrium type of crystals of that polymer. During the high speed rotation of a paddle type of stirrer inside a polymer solution, a flow field is produced which is effective in stretching individual macromolecular coils present in the solution, resulting in the formation of "shish-kebab" fibrillar crystals above certain critical crystallization temperature, T_{cr} ^{25, 43}. The "shish-kebab" structural forms are characterized by the presence of a long fibrillar central trunk (see Figure 2) and laminae grow transversely on this trunk. At temperatures below, T_{cr} , lamellar crystals are formed and this temperature can be considered as the upper limit of chain-folded crystallization.⁴³

There is evidence that when chain folded crystals of a polymer melt or dissolve in a solvent, the nuclei still survive a few degrees^{9, 44, 45} above the apparent melting or dissolution temperature. This stability of the nuclei above the apparent melting or dissolution

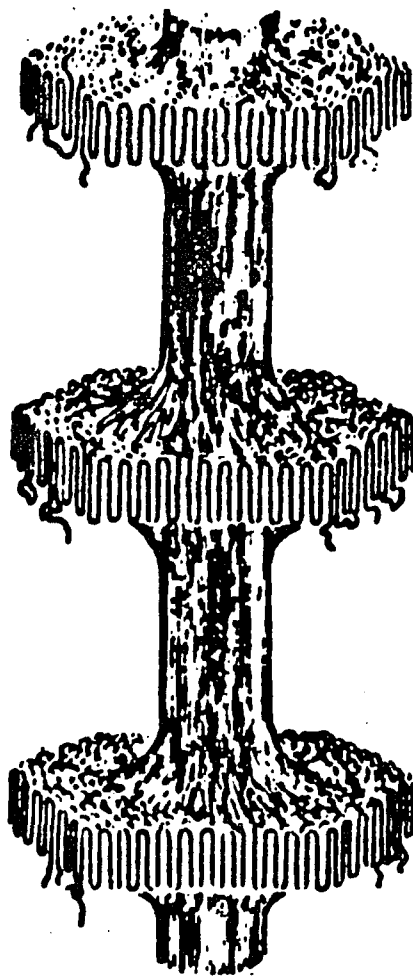


Fig. 2: Schematic representation of a micro shish-kebab indicating the intimate connection of the platelets to the central core.

temperature increases with the increasing molecular weight (\bar{M}_n) of the polymer up to $\bar{M}_n = 10^5$; above this molecular weight, the stability of the nuclei is independent of the molecular weight.

It would be of interest to see whether or not the stabilities of the preformed nuclei can be correlated with the lamellar-to-fibrillar crystal transition temperature.

The efficiency of stirrer-induced crystallization of a polymer is raised if the molecular weight (\bar{M}_n) of the polymer is around 10^5 or higher.⁴³ The high molecular weight fractions of a linear, flexible polymer are more effectively deformed and oriented under the influence of a flow field, produced by the high speed rotation of a paddle type of stirrer inside the polymer solution. So, fractionation of the initial poly-disperse polymer is advantageous for the preparation of stirrer crystals.

The noncrystalline chain traverses present in a stirrer crystallized sample can consist of chain ends, chain folds, interlamellar links and intralamellar defects. Assuming intralamellar defects to be negligibly small,^{15, 29} the noncrystalline fraction is given

$$F_S = (UF + C) / \bar{N}_n \quad (8)$$

where U is the average number of monomer units per fold and interlamellar traverse combined, F is the number of folds and interlamellar traverses per chain with a number average DP of \bar{N}_n , and C is the average number of monomer units in the two chain ends. The crystalline fraction, $1-F_S$, is related to the above parameters and to the crystalline stem length, L_C , by^{15, 29}

$$1-F_S = (L_C / R\bar{N}_n) (F + 1) \quad (9)$$

where R is the crystallographic repeat distance in the chain direction. Equations 1 and 2 can be combined to eliminate F, giving:

$$1-F_S = (L_C/R) \left\{ 1 + (U-C) / \bar{N}_n \right\} / \left\{ U + L_C/R \right\} \quad (10)$$

At large \bar{N}_n , $(U-C) / \bar{N}_n$ will be much smaller than 1 and the crystalline fraction $1-F_S$, will be independent of \bar{N}_n and will be constant with changing \bar{N}_n if L_C and U remain constant. For large \bar{N}_n , Eq. (3) can be written as

$$U = L_C/R \left\{ F_S / (1 - F_S) \right\} \quad (11)$$

L_C can be calculated from the following equation:

$$L_C = \rho_a W_c L / \left\{ \rho_a W_c + \rho_c (1-W_c) \right\} \quad (12)$$

where L is the lamellar thickness.

An estimate of the average length of a non-crystalline chain traverse (in the folds or interlamellar links) can be obtained if the lamellar thickness and the crystallinity (W_c) are known.

For bulk and for dilute solution crystallized TPI, α melts at a higher temperature than β .⁷⁻¹⁵ But for one stirrer-crystallized β - TPI sample Flanagan and Rijke¹¹ reported a melting point around 81°C. This melting point is about 17°C higher than the earlier reported⁸ highest melting point of melt-grown β - TPI crystals and about 7°C higher than the reported highest melting point of α - TPI.⁸ The equilibrium melting point of β - TPI, as evaluated by an extrapolation method involving the measurement of apparent melting point as a function of crystallization temperature^{46, 49} or reciprocal lamellar length⁴⁷, yielded a value of 80°C. So it can be concluded

that the equilibrium melting point of β -TPI is close to 80°C.

The highest melting point of melt-grown α -TPI reported to date is 74°C.^{7, 8} Various values of the equilibrium melting point, as evaluated by extrapolation have been given and include 87°C^{46, 47} and 80°C.^{11, 49} Due to this controversy regarding the equilibrium melting point of α -TPI, no definite conclusion can be drawn regarding the relative stabilities of these two polymorphic modifications.

The evaluation of the equilibrium heat of fusion is difficult, since no absolute values of the enthalpy of amorphous or crystalline polymers are available.⁵⁰ One of the extrapolation methods developed involves the measurement of the heat of fusion as a function of crystallinity and another extrapolation method involves the measurement of melting points in diluent mixtures as a function of concentration.

⁵¹ Hendus and Illers plotted the heat of fusion of polyethylene as a function of specific volume of the sample at room temperature and found a good straight line through the extensive data points. The extrapolated equilibrium heat of fusion is 293 J/g at a specific volume of 1.000 cm³/g for the perfect crystal at room temperature. The accuracy of this extrapolation is supported by the fact that the most perfect crystals produced to date fit the same straight line.⁵⁰ As long as the crystals are not deformed severely by drawing, and the fold length increases sufficiently with increasing crystal perfection, a reasonably good straight line can be drawn through the data points.

Difficulties arise when the crystal perfection, as roughly indicated by the crystallinity or specific volume, and effects of

surface are varied separately. The heat of fusion with the increasing crystallinity of polyethylene samples at constant fold length (about $135\overset{\circ}{\text{A}}$) extrapolates to a heat of fusion 20 J/g lower than 293 J/g. Including the correction for changing crystal perfection, Fischer and Henrichsen⁵² could show that such data lead also to an extrapolated equilibrium heat of fusion of about 293 J/g. Their discussion also includes a detailed evaluation of prior data in the literature.

Recently, this crystallinity extrapolation has been successfully used for the determination of enthalpy change during the solid-solid transition of the two crystal forms of trans -1, 4 - polybutadiene.⁵³ The enthalpy change for the transition is found to be proportional to the specific volume of the majority of the samples.⁵³

No work has been reported to date on the determination of the heat of fusion of either α - and β -TPI by the extrapolation method involving the measurement of heat of fusion as a function of crystallinity.

Calculation of the equilibrium heat of fusion from melting point depression by a diluent is based on the Flory-Huggins equation¹⁷ (See Eq. 5). The advantage of the diluent method is that the percentage crystallinity of the sample does not have to be known. The main difficulties lie with the need to work with crystals which all have the same lamellar size and crystal perfection at the maximum experimental melting temperature.⁵⁰ In the case of β -TPI, there is an additional problem encountered when using the diluent method. In the presence of a diluent, β -TPI converts to α -TPI at temperatures well below the dissolution temperature of the particular β -TPI sample^{7, 14} in the diluent.

8
Mandelkern et al. determined the heat of fusion of α - and β -TPI by the diluent method. Later, Flanagan and Rijke¹¹ also determined the heat of fusion of β -TPI by the diluent method using a stirrer-crystallized sample. There remain considerable uncertainties in the reported values of heat fusion of α and β -TPI. Also neither group of workers^{8, 11} took into account the possibility of a diluent-induced β to α -conversion.^{7, 14}

The intramolecular conformational entropy, ΔS_c , that is gained when a crystalline polymer is melted can be evaluated⁵⁴ by separating from the experimentally observed entropy of fusion ΔS_f^0 the contribution ΔS_v^0 due to the change in volume that occurs on melting:

$$\Delta S_f^0 = \Delta S_v^0 + \Delta S_c \quad (13)$$

The contribution to the entropy of fusion made by the change in volume that occurs on melting can be determined^{55, 56} in the following manner:

$$\Delta S_v^0 = (a/b) \Delta V_f \quad (14)$$

Where a , b and ΔV_f are the thermal expansion coefficient, the compressibility and the volume change on fusion, respectively. a and b can be calculated from pressure - volume - temperature data of the polymer.

8
Mandelkern et al. calculated ΔS_v^0 of α -TPI using equation (13) and an approximate value of b . Also since there are uncertainties in the equilibrium melting point and heat of fusion of α -TPI, ΔS_c calculated from equation (12) is also uncertain. ΔS_c for β -TPI

has not been calculated to date.

ΔS_c can be calculated theoretically from the partition function evaluated by a matrix method,⁵⁷⁻⁵⁹ if the rotational isomeric state theory of the polymer chain is adopted. Tonelli,⁵⁷ and later Naoki and Tomomatsu⁶⁰ calculated ΔS_c of TPI by this method using the statistical weight matrices of Mark⁶¹ and Flory et al.,⁶² respectively; the value is 12 J/mole of repeat unit.

It has been found that β -TPI nucleates faster than α -TPI at all crystallization temperatures.^{14, 63, 64} One of the major factors that determine the nucleation rate is ΔS_c .⁶⁵ If ΔS_c of β -TPI is substantially lower than the α -TPI, then this faster nucleation rate is expected. So the calculation of ΔS_c for α and β -TPI will be important.

Since the fusion of a crystalline polymer is a first order transition, the variation of melting point of that polymer with external pressure can be represented quantitatively by the differential form of the Clausius Clapeyron equation.

$$dT_m^*/dP = T_m^* \Delta V_f / \Delta H_f^0 \quad (15)$$

where ΔV_f is the volume change per repeating unit on fusion of the polymer crystal, and dT_m^*/dP is the pressure coefficient of melting of equilibrium polymer crystal.

ΔV_f and ΔH_f^0 of most substances are not strongly dependent on pressure, especially within a moderate pressure range.⁶⁵ So the pressure coefficient of melting of a substance remain constant within a moderate pressure range.⁶⁶⁻⁷²

For ordinary solid substances, the experimental melting points and the respective equilibrium melting points are identical. But for a crystalline polymer, the experimental melting point varies with the thermal history and unless the polymer crystal is the equilibrium type, the melting point will be lower than the equilibrium melting point of the polymer. However, it has been found experimentally that the pressure coefficient of melting of the equilibrium crystal dT_m^*/dP , is identical to the pressure coefficient of melting of the metastable crystal, dT_m/dP .⁵⁰ Then equation (15) can be written as:

$$\frac{dT_m^*}{dP} = \frac{dT_m}{dP} = \frac{T_m^* \Delta V_f}{\Delta H_f^\circ} \quad (16)$$

If dT_m/dP , ΔV_f and ΔH_f° of a polymer are known, then from equation (16) one can calculate T_m^* . Table II shows the values of dT_m/dP , ΔH_f° , ΔV_f and T_m^* for six polymers and Table III shows the comparison of literature T_m^* with the T_m^* calculated⁷³ using Equation (16) and the data in Table II. It can be seen that T_m^* (calculated) agrees with T_m^* (literature), within reasonable accuracy. Similarly, ΔH_f° of a polymer can be calculated if dT_m/dP , ΔV_f and T_m^* of the polymer is known. Recently Naoki and Tomomatsu⁶⁰ have experimentally determined the value of dT_m/dP for α -TPI and is equal to 36°K/k bar . Since the thermal expansion coefficients of α - and β -TPI and amorphous TPI are known⁹, ΔV_f can be calculated at any temperature. If T_m^* and ΔH_f° values for α -TPI are known, then the reliability of these values can be checked using equation (16).

TABLE II
 Pressure Coefficient of Melting^a, Heat of Fusion^b,
 Volume Change on Fusion^b and Equilibrium Melting Point^c
 Datas of Some Polymers^c.

Polymer	$d T_m/dP$ (°K/kbar)	ΔH_f° (J/g)	ΔV_f (cc/g)	T_m^* (°K)
Polyethylene ⁵⁰	35.0	293	0.2560	415
Polytetrafluoro ethylene ^{50,67 & 71}	152.0	68.3	0.1597	600
Poly trans 1,4- Butadiene ^{50,69,72 & 74}	38.7	77.7	0.0729	415
Polyethylene terephthalate ^{50,68}	47.7	140.7	0.1215	553
Isotatic Polybutene-1, (modification 1) ^{50,78,79}	45.5	125	0.137	414

Table II Continued

Polymer	$d T_m/dP$ (°K/kbar)	ΔH_f° (J/g)	ΔV_f (cc/g)	T_m^* (°K)
Isotactic Polypropylene (modification α) ^{50,70,80,81}	36.6	260	0.211	456

^a Experimentally determined using metastable lamellar crystals at the low pressure regions.

^b At atmospheric pressure.

^c Determined by methods other than using Clausius-Clapeyron Equation.

TABLE III
Comparison of the Calculated^a and Literature Equilibrium
Melting Point

Polymer	T_m^* (literature) (°K)	T_m^* (Calculated) (°K)
Polyethylene	415	415
Polytetrafluoroethylene	600	599
Polytrans-1,4-Butadiene	415	414
Polyethylene terephthalate	553	553
Isotactic Polybutene-1 (modification I)	414	416
Isotactic Polypropylene (α)	456	452

^a Calculated using Clausius Clapeyron equation.

The last important thermodynamic parameter for a crystalline polymer is the equilibrium dissolution temperature. The quantitative interpretation of crystallization of a polymer from solution is hampered by the uncertainty in the magnitude of the equilibrium dissolution temperature. This temperature can be calculated theoretically if the equilibrium melting point and heat of fusion of the polymer and Flory-Huggins interaction parameter and the ratio of molar volumes of polymer and solvent are known.

Experimentally, the equilibrium dissolution temperature can be evaluated by an extrapolation method involving measurements of dissolution temperature of the polymer crystals as a function of crystallization temperature. Another method is the direct determination of dissolution temperature of equilibrium type crystals of the polymer in the particular solvent.

The main difficulties that lie with the extrapolation method for the determination of equilibrium dissolution temperatures of a polymer are the following:

- (i) A large number of data points over a wide range of crystallization temperature are needed,
- (ii) The slow rate of crystallization at higher crystallization temperature, causes good data points to be unavailable
- and (iii) The freezing point of the solvent may lie in the crystallization temperature range thus causing reduction of data points for extrapolation. Sometimes no data points can be obtained.

Flanagan and Rijke¹¹ reported the equilibrium dissolution temperatures of α - and β -TPI in n-butyl acetate to be equal; the equilibrium dissolution temperatures of α - and β -TPI in other solvents have not been reported to date.

The purpose of this work is to obtain new thermodynamic and related parameters for trans-1,4-polyisoprene obtained from solution using quiescent and stirrer crystallization procedures. These thermodynamic parameters are of fundamental importance in describing the physical properties of a polymer and hence more thorough study is important.

STATEMENT OF THE PROBLEM

The major goals of this investigation are the following:

- (1) to obtain more information about the stability of the two crystal modifications of trans-1,4-polyisoprene,
- (2) To carry out a systematic study of the density and the melting point of trans-1,4-polyisoprene crystals stirrer-crystallized from solutions over a wide range of crystallization temperature,
- (3) to study the dissolution of stirrer-crystallized β -TPI in various solvents,
- (4) to obtain by calculation various thermodynamic parameters of the two crystal forms of TPI, such as the equilibrium dissolution temperatures, Flory-Huggins interaction parameter, pressure coefficients of melting and surface free energies.

In order to carry out the calculations in (4) it was necessary to determine the enthalpy of fusions of the two crystal modifications of trans-1,4-polyisoprene by extrapolation of results obtained for specimens of various crystallinities.

During this study the number of monomer units in a non-crystalline chain traverse in fibrous β -TPI was estimated and correlation of crystal form stability with the lamellar-fibrillar transition temperature was found.

EXPERIMENTAL

1. Samples:

Synthetic trans-1,4-polyisoprene (Polysciences, Inc.) Balata (Dunlop) and Gutta Percha (Gabundan Produsen Karet, Indonesia) were used. The Balata and Gutta Percha were purified by repeated precipitation from toluene solution into acetone. The trans 1,4 content was determined by ^{13}C NMR as 99 and 100% respectively, for synthetic polymer and for balata. These determinations were made by F. A. Bovey and F. C. Schilling at Bell Laboratories. Gutta Percha is known to consist exclusively of the trans 1,4 structure.⁷⁵ A Waters GPC 200 instrument was employed to measure the molecular weights^{12,33} of the samples. The \bar{M}_n and \bar{M}_w/\bar{M}_n of unfractionated samples were:

Synthetic TPI	$\bar{M}_n = 3.5 \times 10^4$, $\bar{M}_w/\bar{M}_n = 4.8$
Gutta Percha	$\bar{M}_n = 6.3 \times 10^4$, $\bar{M}_w/\bar{M}_n = 4.3$
Balata	$\bar{M}_n = 1.1 \times 10^5$, $\bar{M}_w/\bar{M}_n = 2.2$

Figure 3. shows the GPC curves for synthetic TPI and Balata samples.

2. Fractionation:

About 10 grams of unfractionated polymer in a 2 liter flask was dissolved in 1 liter of toluene and 0.5 gm. of 2,2'-methylene bis[4-methyl-6-tert-butyl phenol] as antioxidant. Nitrogen gas was passed through the toluene in the flask before the solution was made. The solution was placed in a 28°C bath and agitated while adding methanol to permanent turbidity. A slight excess of methanol was added, then the turbid solution was heated in hot tap water to obtain a clear

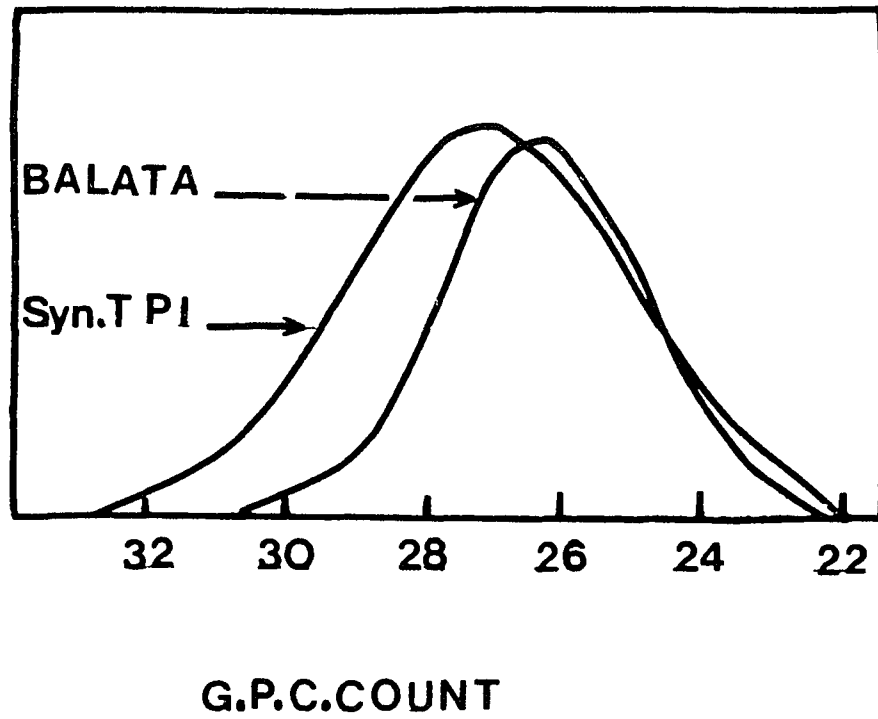


Fig. 3: Gel permeation chromatograms for balata and synthetic trans-1,4-polyisoprene.

solution, immediately replaced in the 28°C bath and allowed to stand overnight. All these operations were done in subdued light. The solution had formed two liquid layers as required for fractionation. The top layer was removed by suction into another flask for further fractionation.^{17,76} The lower layer was precipitated in acetone and dried in a vacuum oven. This was the first fraction.

3. Crystallization:

Prior to crystallization, solutions were prepared by heating the polymer in the solvent for one hour at 80°C. Crystallization was induced in a 2% (W/V) n-butyl acetate or heptane solution of trans 1,4 polyisoprene, TPI, containing antioxidant with a teflon or metal paddle stirrer rotating at a speed of more than 1500 rpm. Crystallization times of 1 to 4 days were used.

Crystallization without stirring was carried out from amyl acetate, n-butyl acetate and heptane solution at constant temperature using various methods at concentrations of 0.3, 0.5% and 1% (W/V). Direct crystallization by rapid cooling from an elevated temperature, T_D , to the final crystallization temperature, T_C , was one method used. Crystallization was also carried out by first rapidly cooling from T_D to 0°C to precrystallize then heating the mixture slowly to a temperature which was chosen as below, as equal to or as above the minimum dissolution (or clearing) temperature. In the cases where redissolution was carried out the solution was cooled quickly to T_C to bring about final crystallization. Following crystallization the precipitate was washed with fresh liquid at T_C and then dried at room

temperature. Melt crystallization was carried out at a slow average cooling rate (7°C/h) after slow heating of the samples to temperatures in the 69–75°C range.

Transformation of the β - to α -form in the presence of a diluent was carried out in glass tubes containing an inert gas.

4. Density Measurements.

Densities were determined in a water-ethanol density gradient column. All samples were pressed at 3.4×10^7 Pa for a few minutes to eliminate air. The weight fraction crystallinity, W_c , was calculated (Eq. 17) assuming a two phase system using an amorphous density,⁹ $\rho_a = 0.905 \text{ gm/cm}^3$ and crystalline densities, ρ_c , of 1.05 and 1.02 gm/cm^3 for α -² and β -TPI³ respectively.

$$W_c = \frac{\rho_c (\rho_s - \rho_a)}{\rho_s (\rho_c - \rho_a)} \quad (17)$$

where ρ_s = density of the sample.

5. Dissolution Temperature Measurements.

Dissolution temperatures of stirrer crystallized β -TPI grown at 48°C from n-butyl acetate, were measured as follows:

Small slices of the samples were immersed in as received reagent grade solvent and heated at an average rate of 1°C per hour. The temperature of disappearance of the last portion of solid was taken as the dissolution temperature. Values were reproducible to 0.5°C.

6. Differential Scanning Calorimetry.

Differential scanning calorimetry (DSC) melting curves were obtained using a DuPont 990 thermal analyzer at a heating rate of 10°C/min. In a few cases a DuPont 1090 thermal analyzer at a heating rate of 10°C/min was also used. The cell constant of each instrument was determined by using indium as standard. The endothermic peak temperatures were taken as the apparent melting points of the samples, after the zero correction for each run.

7. Wide-Angle X-Ray Diffraction.

Wide-angle x-ray diffraction photographs were obtained with a cylindrical camera of 57.3 mm diameter.

RESULTS

1. Stirrer Crystallization of Trans-1,4-Polyisoprene.

Stirrer induced crystallization of trans-1,4-polyisoprene, TPI, was carried out using fractions with $\bar{M}_n = 3 \times 10^5$ and $\bar{M}_w/\bar{M}_n = 1.6$ at a starting concentration of 2 % (w/v) in two solvents, n-butyl acetate and n-heptane, at crystallization temperatures, T_c , and for the time period given in Table IV. The washed and dried products were subjected to wide angle x-ray analysis and to differential scanning calorimetry. Some representative DSC results are given in Fig. 4. The major and minor DSC endotherms are listed for each preparation in Table IV; the crystal form, as determined from the wide angle x-ray results is also given. In two cases ($T_c = 42$ and 46°C , n-butyl acetate) minor endotherms at lower temperatures suggested the presence of some β form mixed with the α form; the minimum amount of the α form for these preparations was estimated from the area under DSC endotherms. The morphology, as given in Table IV, was observed visually and/or using an optical microscope.

In Figs. 5 and 6 the temperature of the highest and most prominent endotherm is plotted vs. crystallization temperature from n-butyl acetate and n-heptane, respectively. The density of most of these preparations is also given in these figures. At the temperature or in the temperature range where a non-fibrous-fibrous morphological change occurs (see Table IV), a discontinuity in the melting

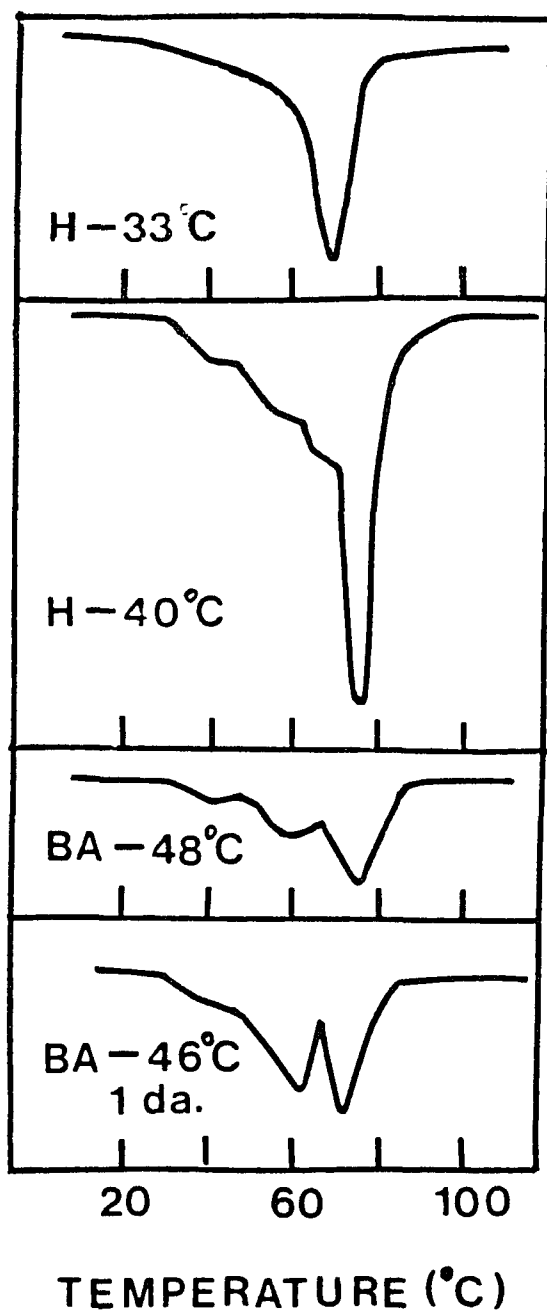


Fig. 4: Differential scanning calorimetry for stirrer-crystallized trans-1,4-polyisoprene at various crystallization temperatures (as given) in heptane (H) and n-butylacetate (BA).

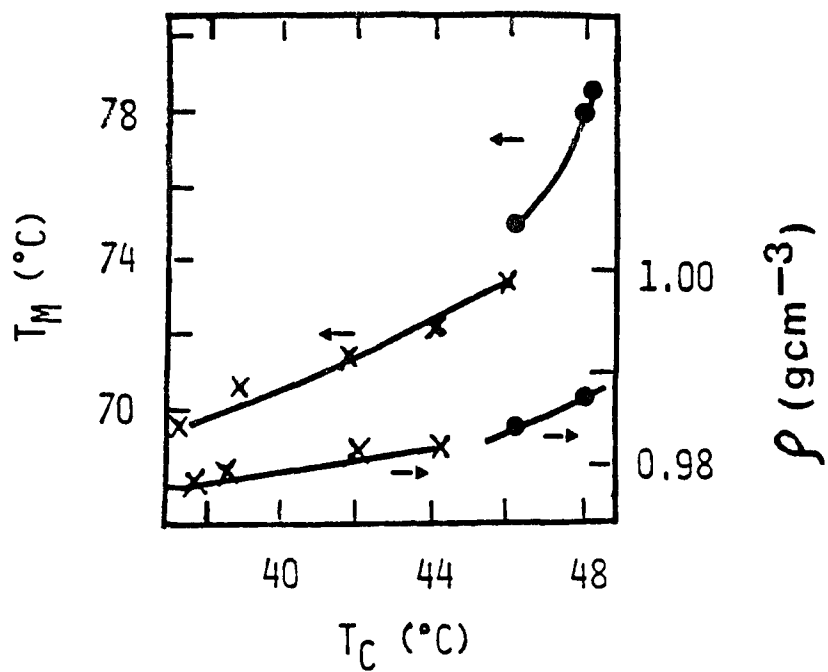


Fig. 5: Melting endotherm T_{ENDO} and density -vs. crystallization temperature for stirrer-crystallized trans-1,4-polyisoprene from n-butyl acetate: (X) nonfibrous, predominantly (>80%) α form; (●) fibrous, β form.

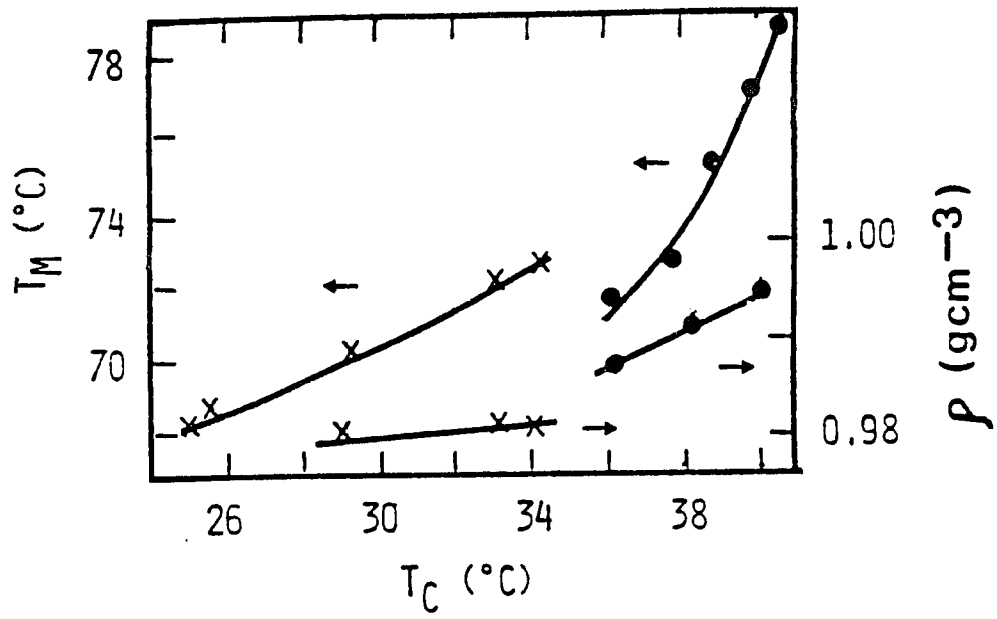


Fig. 6: Same as in Fig. 5 but from n-heptane.

Table IV - Stirrer Crystallization of Trans-1,4-Polyisoprene^a

<u>Solvent</u>	<u>T_c - °C</u>	<u>Time</u>	<u>DSC Endotherm-°C</u>		<u>Crystal</u>	<u>Morphology</u>
		<u>Days</u>	<u>Major</u>	<u>Minor</u>	<u>Form</u>	
n-butyl acetate	38	1	70	-	α	lamellar
	39	1	71	-	α	lamellar
	42	1	72	64,40	> 90% α	lamellar
	44	1	73	62	α	lamellar
	46	1	62,75	40	β	fibrous
	46	4	74	40	> 80% α	lamellar ^b
	48	3-4	60,79	40	β	fibrous
n-heptane	25	1	69	-	α	lamellar
	29	1	70	-	α	lamellar
	33	1	72	-	α	lamellar
	34	1	73	-	α	lamellar
	36	1	55,71	-	β	fibrous
	38	2	72	50	β	fibrous
	40	1	79	64,55,42	β	fibrous

^a $\bar{M}_n = 3 \times 10^5$, $M_w/M_n = 1.6$, concentration -2% (w/v).

^b Three days additional stirring yields a small amount of additional precipitate.

temperature and a change of slope or discontinuity in the density is observed in Fig. 5 and Fig. 6. However, when n-butyl acetate is the solvent, the fibrous β -form sample has a higher endotherm than the non-fibrous α form ($T_c = 46^\circ\text{C}$), while for heptane as solvent a decrease in T_{ENDO} for an increase in T_c from 34°C (α form) to 36°C (β form) is found. The weight fraction crystallinity, as calculated from the density, for the fibrous β form crystallized at various temperatures is given in Table V.

Table V - Crystallinities (W_c) for Stirrer Crystallized β -Trans-1,4 Polyisoprene

<u>Solvent</u>	<u>$T_c - ^\circ\text{C}$</u>	<u>W_c</u>
n-butyl acetate	46	0.71
	48	0.74
n-heptane	36	0.76
	38	0.76
	40	0.78

2. Seeded Crystallization of TPI from n-Butyl Acetate and n-Heptane Solutions.

The effect of temperature on the stability of α -TPI nuclei in n-butyl acetate and n-heptane solution (0.5% w/v) prepared under quiescent conditions was tested with systems containing synthetic polymer with an M_n of 2.5×10^5 and $M_w/M_n = 1.6$. Each sample was

first precrystallized by cooling from 80°C in a constant temperature bath set at 0°C for about a thirty minute period; the mixture was then heated to a redissolution temperature, T_R , just above the minimum dissolution temperature or clearing temperature obtained on slow heating. The results, in terms of the form appearing upon final crystallization, washing of the precipitate and drying at room temperature after heating to T_R , are given in Table VI. Figures 7 and 8 show the effect of the variation of T_R on the melting point, T_m of the seeded crystals. Figure 9 shows some representative DSC melting curves for seeded crystals grown from n-butyl acetate solution. At T_R above 45°C in n-butyl acetate and at T_R above 40°C in heptane the crystal form appearing on final crystallization is β as determined from the wide angle x-ray diffraction photography. Since the apparent melting point of the β -form grown from melt or from solution without stirring at a particular crystallization temperature is lower than the α -form grown under the same condition,¹⁴ Figures 7, 8 and 9 show the drop in melting point when the β -form first forms.

3. Measurement of Heat of Fusion of TPI Crystals using DSC.

Using a differential scanning calorimeter, the heat of fusion was measured for sixteen samples in the β -form, five of which were stirrer crystallized (see above), five were solution crystallized, five were solution crystallized and then annealed at a higher temperature, and one was as received synthetic TPI. When these results are plotted versus the difference in specific volume between

Table VI - Effect of Redissolution Temperature on α -TPI Nuclei^a

<u>Solvent</u>	<u>T_R-°C</u>	<u>Crystal Form</u>
n-butyl acetate	40 to 44	α
	45	α and β
	48 to 60	β
n-heptane	32-35	α
	38-40	($\geq 70\%$) α
	44-50	β

^a $\bar{M}_n = 2.5 \times 10^5$, $M_w/M_n = 1.6$.

the sample and a completely crystalline one, as given in Fig. 10, considerable scatter is observed with the results for the annealed structures showing marked deviations from the other data. A least squares analysis of all sixteen points yields an intercept of 113 Jg^{-1} . A line defined by the stirrer crystallization points has an intercept of 117 Jg^{-1} and this line passes through within experimental error the point for the melt crystallized sample and those for all the solution crystallized samples except one. Therefore the value of ΔH_f° for the β form is taken as 117 Jg^{-1} (8.0 kJ mole^{-1}). The heat of fusion of seven samples in the α form was measured; two of these samples were stirrer-crystallized, two were solution crystallized directly, two were solution-crystallized following precipitation and redissolution, and one was melt crystallized by cooling from 69°C at 7°C per hour. A plot of these results along with data for another

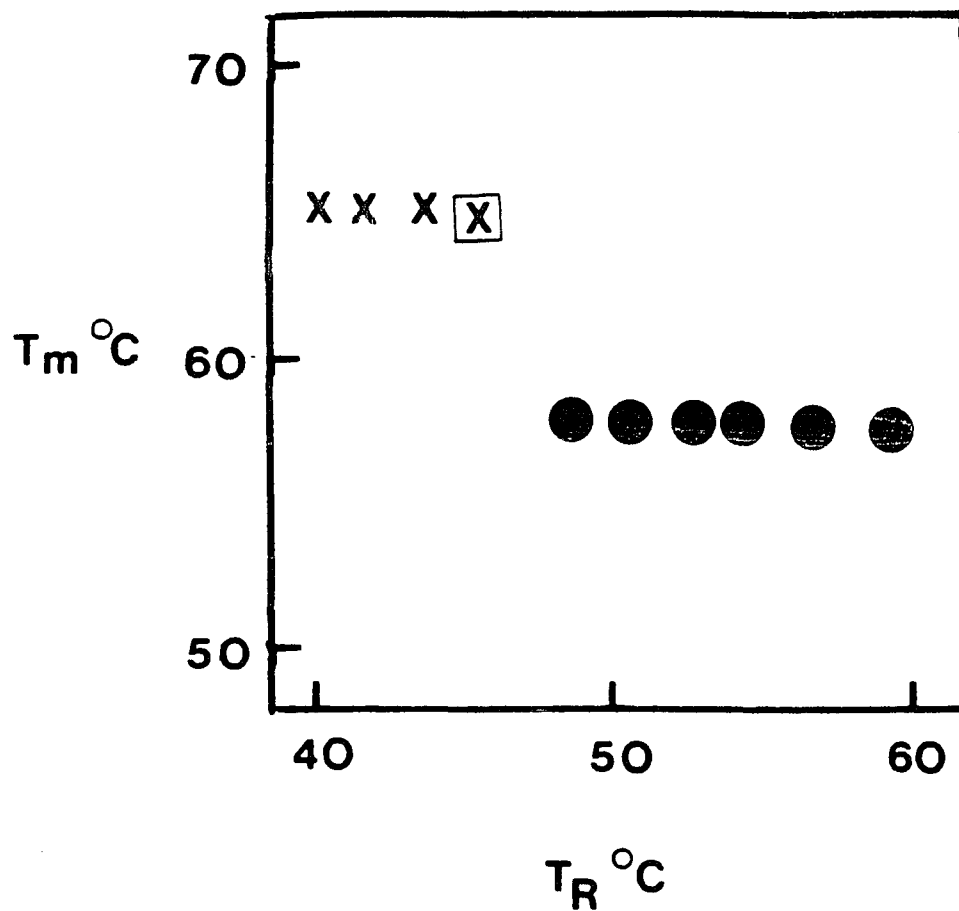


Fig. 7: Effect of variation of T_R on T_m of the seeded crystals grown from n-butyl acetate solution: (X) α -form; (⊠) predominantly α -form; (●) β -form.

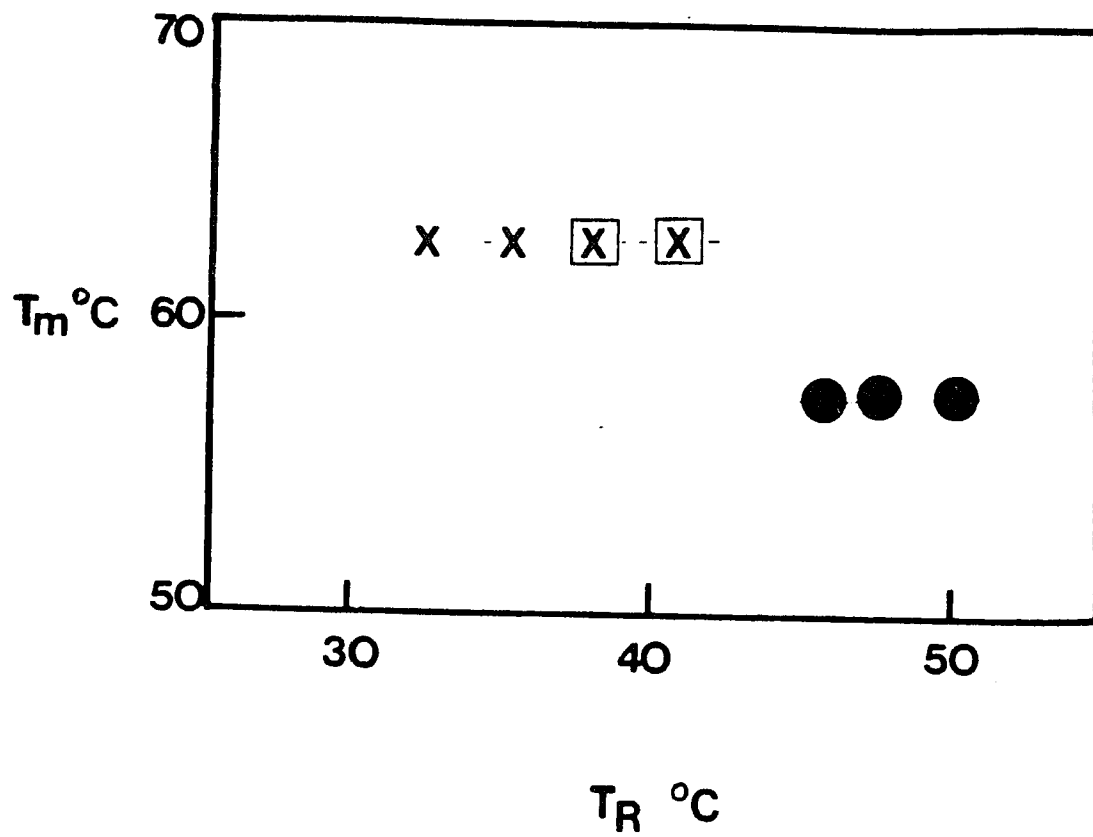


Fig. 8: Same as in Figure 7 but from n-heptane solution.

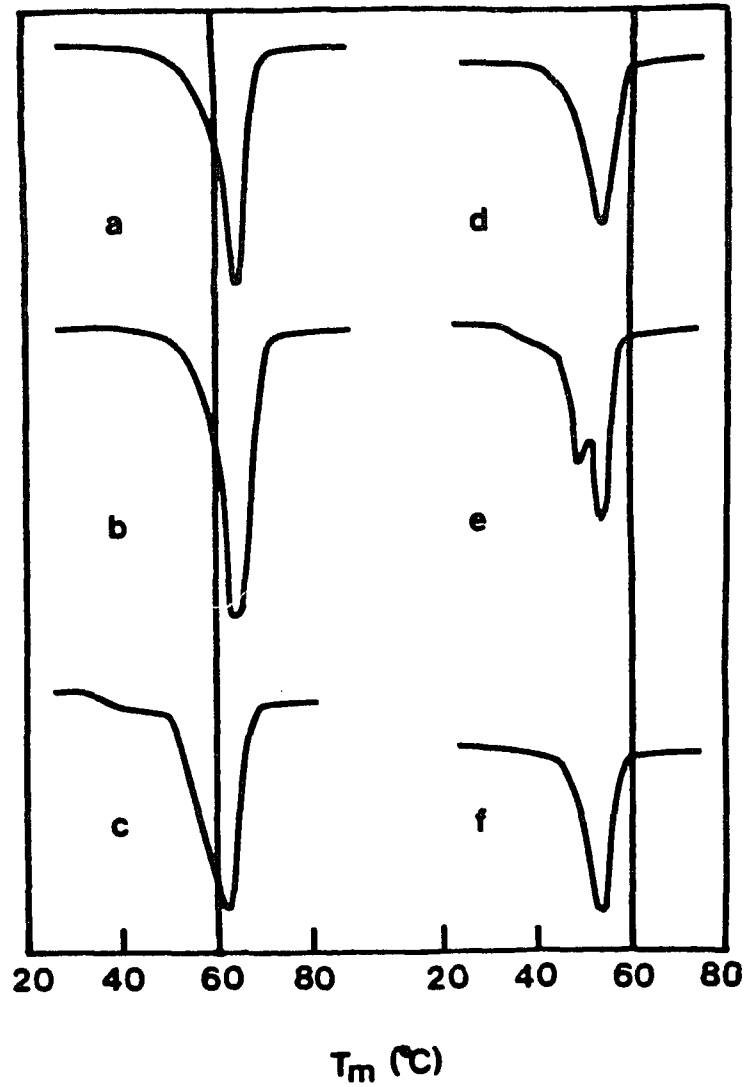


Fig. 9: DSC scans of seeded crystals of TPI (high molecular weight) in n-butyl acetate, at T_R = (a) 42, (b) 44, (c) 46, (d) 48, (e) 49 and (f) 55°C.

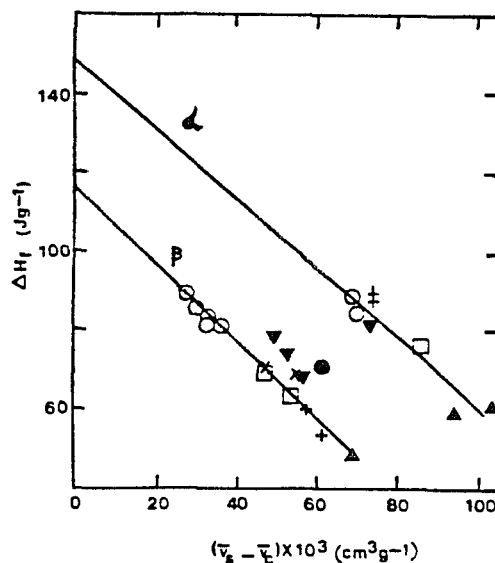


Fig. 10: Heat of fusion for α and β trans-1,4-polyisoprene vs. specific volume difference between the sample and a 100% crystalline sample. α form: (O) stirrer crystallized, (∇) solution crystallized in amyl acetate, 0.3% W/V, unfractionated synthetic, precipitated at 0°C, redissolved at 42°C, $T_C = 10^\circ\text{C}$, (+) solution crystallization in amyl acetate, 1% W/V, $T_C = 30^\circ\text{C}$, $\bar{M}_n = 2.5 \times 10^5$, $\bar{M}_w/\bar{M}_n = 1.3$ and $\bar{M}_n = 1.0 \times 10^5$, $\bar{M}_w/\bar{M}_n = 1.6$, (\square) solution crystallization in amyl acetate, 1% W/V, $\bar{M}_n = 2.5 \times 10^5$ precipitate at 0°C, redissolved at 45°C, $T_C = 10^\circ\text{C}$, (\blacktriangle) melt crystallized (ref.10 and text). β form: (O) stirrer crystallized, (\square) solution crystallized, n-butyl acetate or n-amyl acetate 0.3% W/V, $T_C = 0^\circ\text{C}$, unfractionated synthetic, (X) same but annealed at 20°C for 12 hrs in crystallization liquid, (+) solution crystallized, amyl acetate, 1% W/V, $\bar{M}_n = 2.5 \times 10^5$, $\bar{M}_w/\bar{M}_n = 1.3$ or $\bar{M}_n = 1.0 \times 10^5$, $\bar{M}_w/\bar{M}_n = 1.6$ $T_C = 0^\circ\text{C}$, (\bullet) same but $T_C = 10^\circ\text{C}$, $\bar{M}_n = 2.5 \times 10^5$ only, (∇) same, $T_C = 0^\circ\text{C}$ but annealed in crystallization liquid at 10, 20 or 30°C; (\blacktriangle) synthetic pellet as received.

melt-crystallized sample⁶⁰ yields a ΔH_f° of 149 Jg^{-1} (10 kJ mole^{-1}). The preparation condition, form, density, weight percentage crystallinity and heat of fusion of the samples are listed in Table VII. Fig. 11 shows some of the heat of fusion curves for TPI samples.

4. Effect of Diluents on the Conversion of β to α Form.

The effect of the presence of a swelling agent on the β to α conversion in TPI was studied using the following: heptane, n-butyl acetate, amyl acetate, and mixtures of amyl acetate and toluene and of ethyl acetate and toluene. In these experiments pellets of synthetic unfractionated TPI were used as received or pressed into platelets at 56°C . The principal DSC endotherm for these samples was at 47° and 49°C , respectively, and both the samples were found to be in the β form as determined by wide-angle x-ray diffraction photography. DSC plots before and after swelling with n-butyl acetate at 25°C for one day are shown in Figure 12; it can be seen that the swelling treatment causes a shift of the endotherm from 49° to 61°C . After swelling and drying, this sample was found by wide angle x-ray diffraction to be in the α form. The results for pellets swollen with n-butyl acetate and the other liquids used are summarized in Table VIII, in which the swelling time and temperature, the diluent volume fraction (given approximately in all but one case), and the DSC endotherm(s) observed are shown. In all experiments the TPI sample remained opaque and retained its general shape throughout the swelling period. For the sample swollen in amyl acetate at 35°C the secondary endotherm at 68°C

Table VII. Preparation Condition, Polymorphic Modification, Density (at 25°C), Crystalline Fraction (W_c) and Heat of Fusion of α - and β -TPI Samples.

Preparation Condition of TPI Crystal	Form ^a	Density (g/cc)	W_c	ΔH_f (Exp) (J/g)
1. Dilute Solution grown; $c = 0.3\%$ (w/v) TPI/n-butyl acetate; $T_D = 100^\circ\text{C}$; $T_c = 0^\circ\text{C}$.	β	0.968	0.58	63 ± 2
2. Same as above, but the wet crystals were annealed in the presence of solvent for 12 hours at 20°C	β	0.966 $\pm .002$	0.56	68 ± 2
3. Same as #1 above but the solvent was amyl acetate	β	0.975	0.62	69 ± 3
4. Same as #3 above but treated like #2	β	0.974 $\pm .002$	0.63	70 ± 3
5. Bulk synthetic TPI (as supplied)	β	0.954	0.46	48 ± 2

Table VII. Continued

Preparation Condition of TPI Crystal	Form ^a	Density (g/cc)	W _c	ΔH _f (Exp) (J/g)
6. Stirrer Crystallized; Balata first fraction (M _n = 3 x 10 ⁵), c = 2% (w/v) n-butyl acetate as solvent, T _c = 46°C, 1 day stirring	β	0.984 ±.002	0.71	82 ± 3
7. Stirrer Crystallized; Same as #6, but T _c = 48°C and 3 days stirring	β	0.987 ±.002	0.74	82 ± 2
8. Stirrer crystallized same as #6 but the solvent was heptane and T _c = 36°C	β	0.987 ±.002	0.74	84 ± 2
9. Same as #8, but T _c = 38°C	β	0.987 ±.002	0.74	84 ± 2

Table VII. Continued

Preparation Condition of TPI Crystal	Form ^a	Density (g/cc)	W _c	ΔH _f (Exp) (J/g)
10. Same as #9, but T _c = 40°C	β	0.992 ±.002	0.78	90 ± 2
11. Solution crystal- lized, amyl acetate, c = 1% w/v, $\bar{M}_n = 2.5 \times 10^5$, $\bar{M}_w/\bar{M}_n = 1.3$, T _c = 0°C	β	0.960	0.50	55 ± 3
12. Same as 11, but $\bar{M}_n = 1.0 \times 10^5$, $\bar{M}_w/\bar{M}_n = 1.6$	β	0.966	0.56	60 ± 3
13. Same as 11, but T _c = 10°C	β	0.966	0.56	68 ± 3
14. Same as 11, but annealed at 10°C in amyl acetate	β	0.968	0.58	69 ± 3
15. Same as 14, but annealed at 20°C	β	0.971	0.60	75 ± 3
16. Same as 14, but annealed at 30°C	β	0.977	0.63	78 ± 3

Table VII. Continued

Preparation Condition of TPI Crystal	Form ^a	Density (g/cc)	W _c	ΔH_f (Exp) (J/g)
17. Stirrer crystallized sample from n-butyl acetate; TPI first fraction, c = 2% w/v, T _D = 100°C, T _C = 38°C	α	0.978	0.54	84 ± 3
18. Dilute solution grown, syn. TPI/amy1 acetate, c = 0.3% w/v, T _D = 100°C, T _P = 0°C, T _R = 42°C; T _C = 20°C	α	0.976	0.52	82 ± 3
19. Same as #11, but the solvent was heptane and T _C = 25°C	α	0.980	0.57	88 ± 3
20. Melt grown, unfrac- tioned Gutta percha, cooled down to room temperature from an initial temperature of 100°C in vacuum; cooling rate 0.1°C/hr. Reference (40)	α	0.956	0.36	59 ± 2

Table VII. Continued

Preparation Condition of TPI Crystal	Form ^a	Density (g/cc)	W _C	ΔH _f (Exp) (J/g)
21. Same as #14, but the initial temperature was 69°C, the cool- ing rate was 7°C/hr and the sample was Balata first fraction	α	0.947	0.32	60 ± 3
22. Solution crystal- lization in amyl acetate 1% w/v, T _C = 30°C, M _n = 2.5 × 10 ⁵ , M _w /M _n = 1.3	α	0.975	0.52	88 ± 3
23. Same as 22, but M _n = 1.0 × 10 ⁵ , M _w /M _n = 1.6	α	0.975	0.52	86 ± 3
24. Solution crystal- lization in amyl acetate, 1%, w/v, M _n = 2.5 × 10 ⁵ , precipitate at 0°C, redissolved at 45°C, T _C = 10°C.	α	0.96	0.49	76 ± 3

^a As determined by wide angle x-ray photography and DSC melting curves

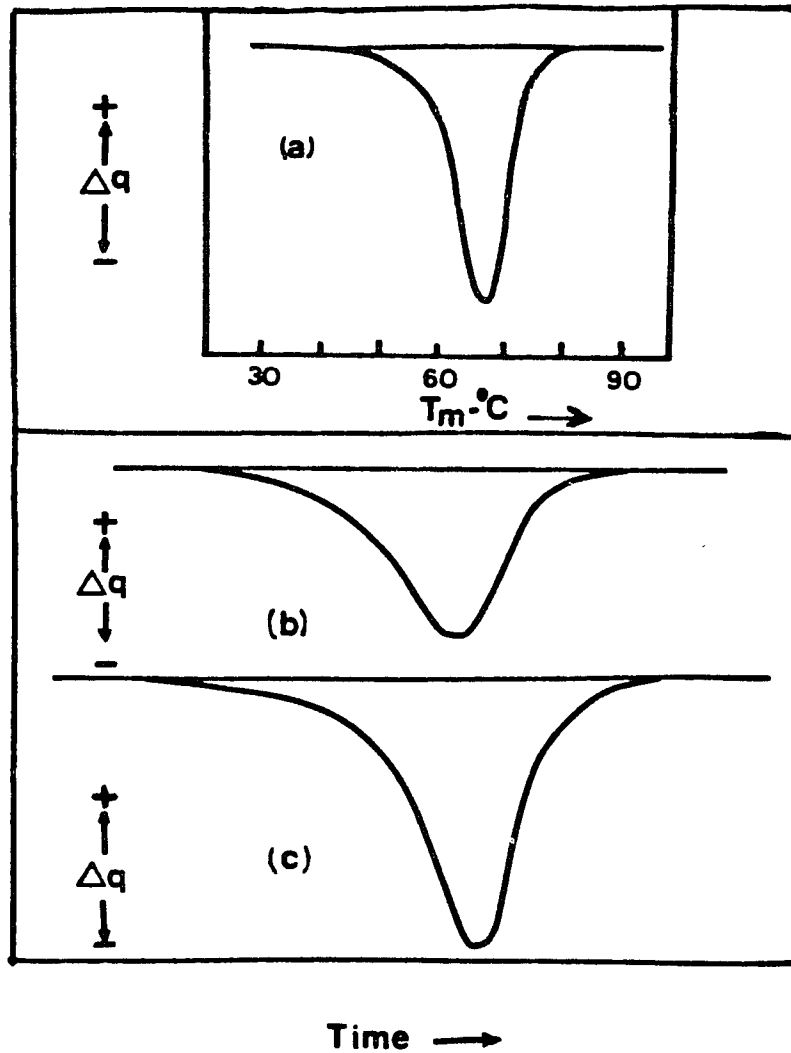


Fig. 11: Some examples of heat of fusion curves for TPI samples:
 (a) α -TPI (Dupont 1090 instrument); (b) β -TPI and
 (c) α -TPI (Dupont 990 instrument). Sample size:
 (a) approx. 10 mg, (b) and (c) approx. 4 mg were used.

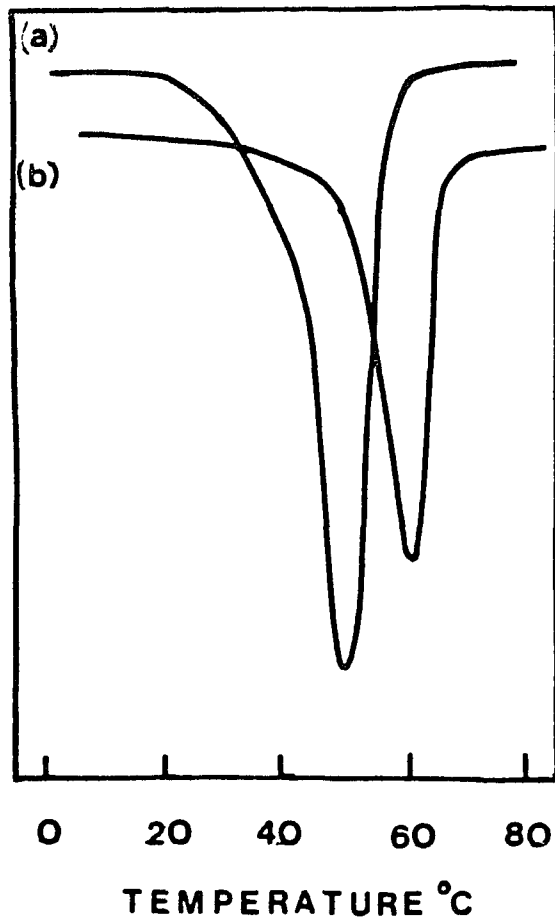


Fig. 12: DSC scans for synthetic TPI pressed at 56°C, (a); pressed at 56°C and swollen for 1 day at 25°C in n-butyl acetate and dried, (b).

Table VIII. Effect of Diluents on the DSC Endotherm for TPI

Treatment	Liquid	Diluent		<u>Endotherms (°C)</u>	
		volume fraction	volume	Major	Shoulders
None	---	---		47	51,40
Swollen for 3 days at 25°C	Heptane	0.1 - 0.2		66	---
	Amyl acetate(2): toluene (1)	0.1 - 0.2		65	---
	Ethyl acetate(2): toluene (1)	0.1 - 0.2		68	---
Swollen at 35°C for 17 hr	Amyl acetate	0.1 - 0.2		60	68
	n-butyl acetate	0.1 - 0.2		60	---
Pressed at 56°C	---	---		49	---
Pressed at 56°C; swollen 1 day at 25°C	n-butyl acetate	0.14		61	40

was prominent. The DSC results show that in all of these experiments a β to α transformation has taken place; this effect was reported earlier by Leeper and Schlesinger.⁷

5. Measurement of Dissolution Temperature of Stirrer Crystallized β -TPI in Various Solvents and Calculation of Equilibrium Dissolution Temperature.

The dissolution temperature of β -TPI, stirrer crystallized in n-butyl acetate at 48°C was measured in thirteen liquids and was found to vary from 29.0 to 65.0°C. The equilibrium dissolution temperature, T_D^* , can be calculated using the equation (6)¹⁸

$$(1/T_D^*) - (1/T_m^*) = (R/\Delta H_f^\circ)(1/x)(1/\chi) \quad (6)$$

where T_m^* is the equilibrium melting temperature, R the universal gas constant, ΔH_f° the heat of fusion per mole of repeat units, x the ratio of solvent molar volume to polymer repeat unit molar volume and χ the Fory-Huggins Interaction Parameter. T_D^* was calculated as given in Table IX for the α - and β - forms of TPI in liquids for which χ values were available. T_m^* values of 353°K for α and 356°K for β

Table IX - Dissolution Temperature for Trans 1,4 Polyisoprene^a

<u>Solvent</u>	χ	<u>ref</u>	$T_D^* - ^\circ\text{C}$ <u>(Calc)</u> ^b		$T_D - ^\circ\text{C}$ <u>(Exp)</u>
Toluene	0.36	77	38	30	37
CCl ₄	0.28	77	32	23	29
Cyclohexane	0.22	76	33	26	36

Table IX Continued

<u>Solvent</u>	χ	ref	$T_D^* - ^\circ\text{C}$ <u>(Calc)^b</u>		$T_D - ^\circ\text{C}$ <u>(Exp)</u>
Benzene	0.52	77	44	37	33
n-Butyl acetate	0.61	11	59	55	58

^a obtained by stirrer crystallization in n-butyl acetate at 48°C

^b from equation 6

were used.¹¹ The ΔH_f° values employed were 8.0 kJ mole⁻¹ for β , as obtained in this work, and 10.5 kJ mole⁻¹ for α (reference 11). T_D values obtained experimentally with stirrer crystallized β -TPI are also given in Table IX. For four of the five solvents the experimental T_D is in agreement to within three degrees with T_D^* for α -TPI. If it is assumed that the experimental T_D values are equal to the T_D^* 's for the α -form, equation 6 can be used to calculate χ as given in Table X. Combination of equations 6 for the α and β forms and eliminating x and χ allows the calculation of T_D^* for the β form from the experimental T_D values so obtained are given in Table X.

Table X. Values of χ and T_D^* for β -TPI Calculated from T_D (Exp)

Solvent	T_D (Exptl.) (°C)	χ^a	$T_D^*(\beta\text{-TPI})^a$ (°C)
Toluene	37.0	-	29
CCl ₄	29.0	-	19
Cyclohexane	35.5	-	27
Benzene	33.0	0.36	24
n-Butyl Acetate	58.5	-	55
Amyl Acetate	58.0	0.54	55
Heptane	52.0	0.45	47
Hexanes	51.5	0.48	47
Dodecane	58.0	0.29	55
Tetradecane	62.0	0.34	60
Methyl Oleate	65.0	0.29	64
Tetrahydrofuran	40.5	0.52	33
Xylenes	44.5	0.36	38

^a Calculated from equation 6.

6. Crystallization of TPI From the Melt.

Crystallization of synthetic TPI not in contact with the liquid was carried out at slow average cooling rates (7°C/h) after slow heating of the samples to temperatures one degree apart in the 70 - 75°C range. From the DSC results given in Figure 13, it can be seen that only the α -form is nucleated when the starting sample temperature is

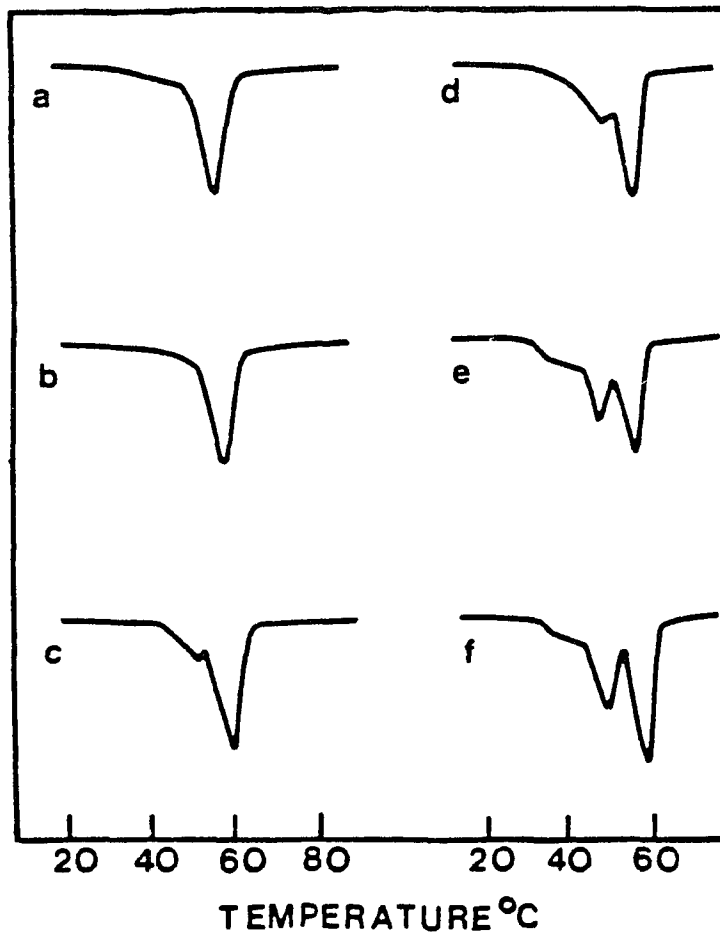


Fig. 13: DSC scans for synthetic TPI cooled slowly (average rate $7^{\circ}\text{C}/\text{h}$) from (a) 70°C , (b) 71°C , (c) 72°C , (d) 73°C , (e) 74°C , and (f) 75°C .

70°C. As this starting temperature is increased, an endotherm characteristic of the β -form appears and increases in size. Quenching to 0°C from a starting temperature of 80°C results in only the β -form crystallizing, as determined by DSC and wide angle x-ray diffraction photography.

7. Calculation of the Pressure Coefficient of Melting of α - and β -TPI.

The ΔH_f° and T_m^* values employed to calculate the pressure coefficient of melting of α - and β -TPI are listed in Table XI. The pressure coefficient of melting is calculated using the Clausius Clapeyron Equation:

$$dT_m^*/dp = T_m^* \Delta V_f / \Delta H_f^\circ \quad (15)$$

where ΔV_f is the volume change per repeating unit on melting as obtained from the literature.⁹ Values of dT_m^*/dp of 38 and 43°K kilobar⁻¹ are calculated for the α and β -forms, respectively.

Table XI - Values of ΔH_f° and T_m^* for α and β -TPI^a

	α -TPI	β -TPI
ΔH_f° (kJ/mol r.u.)	10.5	8.0
T_m^* (°K)	353	356

^a These same T_m^* and ΔH_f° values of α and β TPI were used to calculate T_D^* of α and β -TPI.

8. Recalculation of the Surface Free Energies of α and β -TPI.

The same ΔH_f° and T_m^* values listed in Table XI were also used to recalculate values of the surface free energy for α - and β -TPI using the equation³⁰⁻³²

$$T_m = T_m^* (1 - 2 \sigma_e / \Delta H_f^\circ L) \quad (7)$$

$$\text{or, } \sigma_e = L \Delta H_f^\circ (T_m^* - T_m) / 2 T_m^* \quad (7')$$

where L is the lamellar thickness. L and T_m values for α - and β -TPI found experimentally for melt-crystallized samples⁴⁸ were employed in these calculations, (see Table XII). Values of 42 ± 1 and 53 ± 1 ergs cm^{-2} , respectively, were obtained for σ_e for α and β -TPI. Values of L at T_m 's above those measured by Long and Davies⁴⁸ were calculated

Table XII. Melting Points, T_m , and Lamellar Lengths, L , of Melt-Grown TPI (Purified Gutta percha, $\bar{M}_v = 3.85 \times 10^5$) at Various Crystallization Temperatures, T_c .⁴⁸

T_c ($^\circ\text{C}$)	T_m ($^\circ\text{C}$)		L (\AA)	
	α -TPI	β -TPI	α -TPI	β -TPI
40	-	53	-	106
45	61	57	100	118
50	63	59	107	130
55	65	62	118	150

from equation 7' for the α and β forms as shown in Fig. 14. The two curves are found to cross at $T_m = 76^\circ\text{C}$.

9. Estimation of Average Length of a Non-Crystalline Chain Traverse in the Fibrous β -TPI.

If it is assumed that the fibrous structures with the β -crystal form prepared by stirrer crystallization are made up of alternating crystalline and non-crystalline (amorphous) sections then it is possible to obtain an estimate of the average length of a non-crystalline chain traverse (in the folds or in interlamellar links) from the lamellar thickness and the crystallinity ($W_c = 1 - F_s$) using the following equation.^{15,29}

$$U = (L_c/R) (1 - W_c)/W_c \quad (11)$$

where R is the crystallographic repeat distance along the chain direction; for β -TPI it is 0.475 nm.³ L_c is the crystalline stem length and can be calculated from the lamellar thickness, L, using^{15,29}

$$L_c = \rho_a W_c L / \rho_a W_c + \rho_c (1 - W_c) \quad (12)$$

where ρ_a and ρ_c are the noncrystalline⁹ and crystalline densities,³ respectively. The L value for the stirrer crystallized structures was obtained from Figure 14. For the maximum T_{ENDO} measured (79°C)

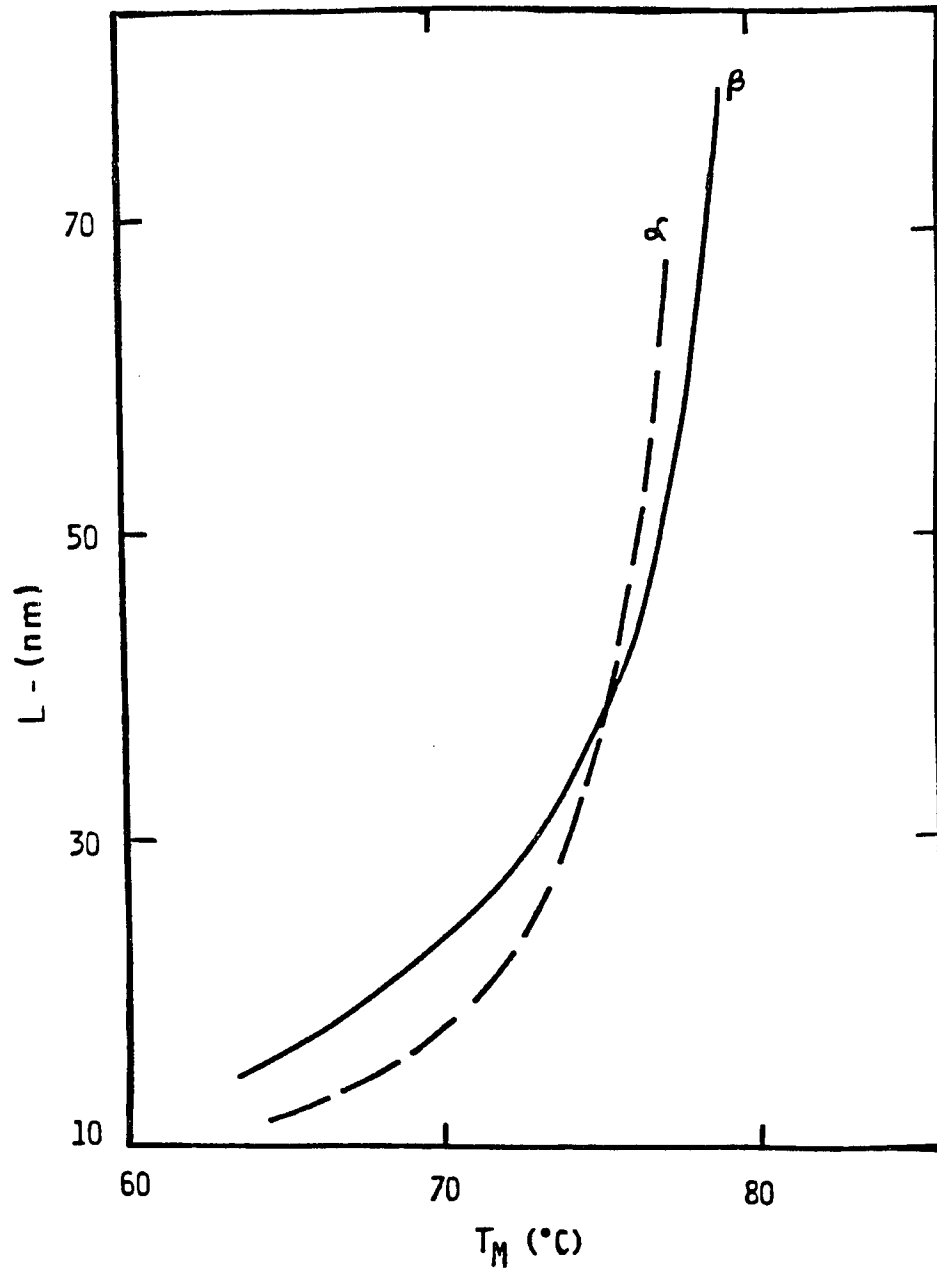


Fig. 14: Lamellar thickness (L) vs. melting temperature (T_m) for α and β -TPI.

and assuming $T_m = T_{\text{ENDO}}$, L is 78 nm, L_c is 59 nm and U is 36 monomer units per noncrystalline traverse.

10. Calculation of the Entropy of Fusion of α - and β -TPI.

The entropy of fusion of a solid substance can be calculated from equation (1),

$$\Delta S_f^\circ = \Delta H_f^\circ / T_m^* \quad (1)$$

Taking ΔH_f° and T_m^* values of α - and β -TPI from Table XI and using equation (1), ΔS_f° of α -TPI is calculated to be 30 J/deg./repeating unit or 10 J/deg/flexible chain unit and for the β -TPI the entropy of fusion, ΔS_f° , is calculated to be 22 J/deg/repeating unit or 7 J/deg/flexible chain unit.

If one assumes that volume expansion and conformational randomization are the steps in melting then the entropy change on expansion to the liquid volume can be calculated from the following thermodynamic relations:

$$\Delta S_v^\circ = (a/b)\Delta V_f \quad (8)$$

where a and b are the expansion coefficient and the isothermal compressibility, respectively.

Mandelkern et al.⁸ estimated ΔS_v° of α -TPI to be 15 J/degree/mole repeat unit using approximate values of a, b and ΔV_f of α -TPI.

Using the recent literature values of b, a^{60} and $\Delta V_f, \Delta S_v^{\circ}$ can be calculated to be 21 and 18 J/deg/mole r.u., for α and β -TPI respectively.

11. X-Ray Diffraction Measurements of α - and β -TPI.

The interplanar spacings (d) and relative intensities of α - and β -TPI crystals as obtained from wide-angle x-ray diffraction photography are listed in Table XIII.

TABLE XIII. X-Ray Diffraction Measurement of α - and β -TPI Interplanar Spacings and Relative Intensities

SAMPLE β -TPI				SAMPLE α -TPI			
Experimental		Literature ¹		Experimental		Literature ¹	
d (Å)	I ^a	d (Å)	I ^a	d (Å)	I ^a	d (Å)	I ^a
-	-	-	-	7.80	M	7.91	M
4.72	VS	4.73	VS	4.90	VS	4.95	VS
3.90	VS	3.92	VS	3.88	VS	3.95	VS
-	-	-	-	3.33	S	3.36	VS
2.95	VW	2.98	MW	2.95	W	2.95	MW
2.37	W	2.38	M	-	W	2.47	VW
-	-	-	-	2.30	W	2.29	W
Not measured	-	1.93		Not measured	-	2.03	VW

^a = visual estimation of relative intensity;

W = weak, M = medium

S = strong, and VS = very strong

The listed d-spacings agree with the literature¹ d-spacings.

DISCUSSION

Previous work has shown that upon heating solid melt-crystallized β -TPI in the absence of diluents, fusion occurs in the 60-65°C range.⁸ If the β form is then nucleated it will crystallize at or somewhat above the β fusion temperature.¹⁰ In the present work in which the β form is transformed to the α -form in the presence of a liquid, the crystallinity was not completely destroyed; therefore, a direct transformation from the β to α form is taking place. The surface free energy for the fold surfaces of the β form has been found to be lower than that for the α -form. Apparently, a liquid at the crystal surfaces can lower the surface free energy, thus bringing about the β to α transformation.

The occurrence of this diluent-induced transformation of β to α should be of considerable importance in determining the polymorphic composition during the crystallization of TPI from solution; the occurrence of this transformation could also affect the results of experiments on β -TPI in the presence of diluents.

In an earlier study⁸ the heat of fusion ΔH_f° was found to be 13 ± 1 kJ mole⁻¹ and 8 ± 2 kJ mole⁻¹, respectively, for α - and β -TPI. From the present study the value for α -TPI is about 20% lower and for β -TPI it is in agreement. Some thermodynamic parameters for trans-1,4-polyisoprene prepared by stirrer induced crystallization in n-butyl acetate at 49°C have also been reported by Flanagan and Rijke.¹¹ The melting temperature measured dilatometrically was found to be 81°C, the dissolution temperature in n-butyl acetate 58°C, and the

equilibrium heat of fusion measured using n-butyl acetate as a diluent $10.5 \text{ kJ mole}^{-1}$. The equilibrium dissolution temperature of α -TPI in n-butyl acetate as measured by the extrapolation method involving crystallization temperature as a function of dissolution temperature was also reported¹¹ to be 59°C . The maximum DSC endotherm found in this work for stirrer crystallized TPI in n-butyl acetate and in heptane of 79°C is not directly comparable with the melting temperature from dilatometry, due in part to the non-equilibrium nature of DSC and to T_{ENDO} occurring above the apparent melting temperature. The dissolution temperature in n-butyl acetate found in the two studies agree. From evidence in the present study, it appears that a β to α transformation occurred during the measurement¹¹ of ΔH_f° due to the use of a diluent; therefore the value of ΔH_f° obtained starting with stirrer-crystallized β -TPI is actually for α -TPI. For the following reasons a ΔH_f° value of $10.5 \text{ kJ mole}^{-1}$ for α -TPI is used in calculating other thermodynamic properties in this work: 1) this value was obtained by an equilibrium measurement, 2) the value obtained by DSC required a large extrapolation and was found using a small number of data points, and 3) better agreement between calculated and experimentally derived quantities occurs.

As noted earlier for polyethylene,⁴³ stirrer crystallization leads to a fibrous precipitate above a certain temperature and folded chain structures below that temperature. However for trans-1,4-polyisoprene the crystal form that appears above and below this temperature is usually different, although in one case this appears to be

concentration dependent (n-butyl acetate at 46°C). The lowest temperature at which fibrous TPI crystallized from n-butyl acetate (2% w/v; $\bar{M}_n = 3 \times 10^5$) upon stirring (46°C) is about equal to that at which preformed nuclei in unstirred solution (0.5% w/v) disappear (45°-47°C). When n-heptane is used as crystallization solvent, the lowest temperature for the preparation of the fibrous β -TPI ($\bar{M}_n = 3 \times 10^5$) is 36°C while the preformed α -nuclei apparently disappear at 41-44°C. The precipitation of the non-fibrous α -TPI under stirrer-induced crystallization takes place at a much faster rate than for non-stirred crystallization presumably due to an increased rate of mass transfer during the stirring process. This therefore makes larger lamellar thicknesses, higher melting endotherms and larger crystallinities more easily attainable. For example, for lamellas crystallized from amyl acetate at a T_c of 32°C ($\bar{M}_n = 2.5 \times 10^5$, concentration = 1% w/v) a melting endotherm of 67°C and a crystallinity of 0.52 were obtained^{12,14} as compared to values of 70-74°C and 0.57-0.59 for stirrer crystallized lamellas (n-butyl acetate, $T_c = 38$ -43°C).

In Fig. 15 the results for stirrer crystallization of TPI from n-butyl-acetate at various temperatures are schematically represented in terms of the crystal modification and morphology present. Similar schematic diagrams can be drawn for other TPI/solvent systems. At crystallization temperatures above 45°C, β -TPI in a fibrous form was recovered. Although the equilibrium dissolution temperature of β -TPI in n-butyl acetate is lower than that of α -TPI, (see Table IX) β -TPI fibrous crystals formed from the solution probably because a lower conformation entropy change is required to generate β -nuclei.⁶⁵ To

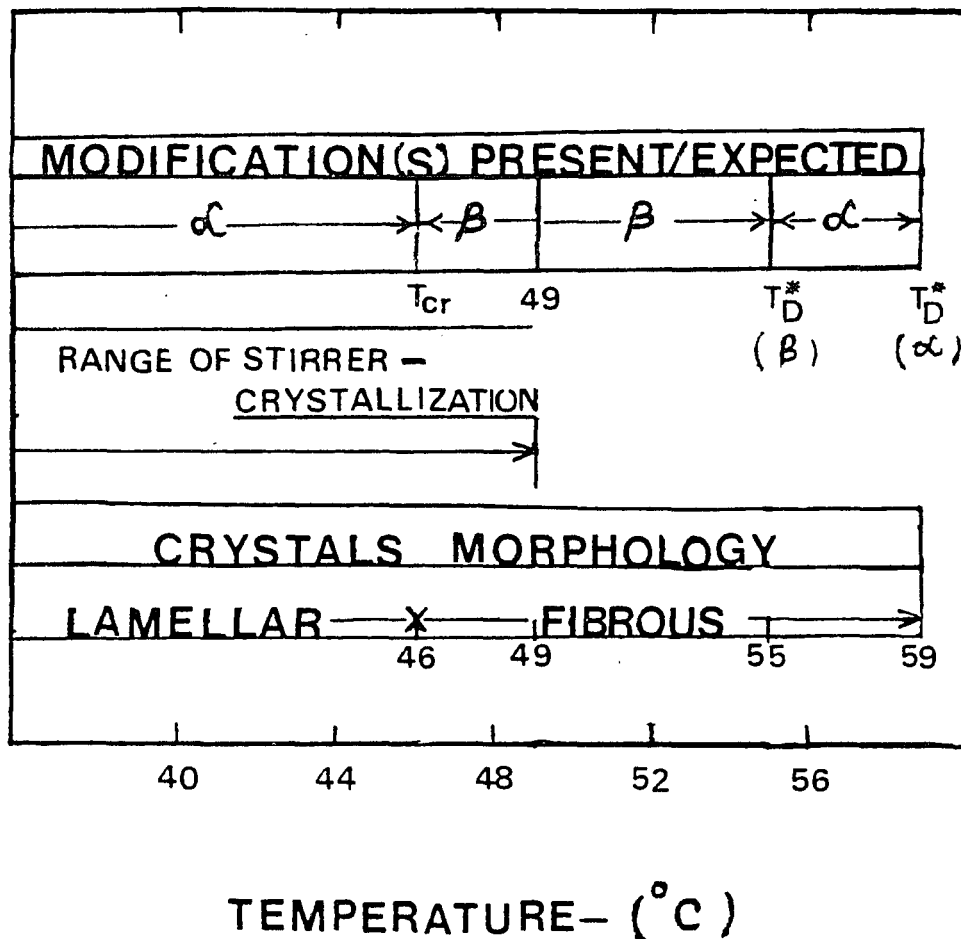


Fig. 15: "Crystallization Scale" showing the temperatures at which various types of crystallization, morphology and polymorphic modifications can occur from n-butyl acetate solutions of TPI. T_D^* is the equilibrium dissolution temperature, T_{cr} is the upper limit of lamellar crystallization.

prepare extended chain crystals of α -TPI from n-butyl acetate solution one has to crystallize at a temperature above 55°C but below 59°C; the latter temperature being the equilibrium dissolution temperature of α -TPI in n-butyl acetate. The apparent dissolution temperature of stirrer-crystallized β -TPI is found to be 59°C. This finding indicates that the final product dissolved in n-butyl acetate is extended-chain crystals of α -TPI formed from the β -TPI stirrer crystals in the presence of diluent and slow heating. Therefore this method can be used to prepare α -TPI in the extended form.

When TPI is crystallized from solution without stirring^{14,15} (T_c of 10°C) or from the melt²⁸ (T_c of 56-65°C) T_{ENDO} for the α form is larger than for the β form. However, for samples prepared by stirrer crystallization from n-butyl acetate and in some cases from n-heptane this does not hold (see Figs. 5 and 6) if a linear extrapolation of the T_{ENDO} vs T_c lines are made. At T_{ENDO} 73°-74°C this quantity for the β form exceeds that for the α form at a particular T_c . The temperature 74°C was taken earlier¹⁴ as that at which the α and β forms are equally stable with β being thermodynamically stable above that temperature and stable below. The β modification can be formed below 74°C due to a faster nucleation rate.¹⁴ Transformation of β to α can occur below 74°C with or without a swelling agent. The relative ease of nucleation of the β form may be due to the fact that this crystal structure is more extended than the α structure. The appearance of two or more endotherms for the fibrous β structures suggest the formation of shish-kebob structures⁴³ with the fibrous parts having the larger T_{ENDO} and the lamellar overgrowths the lower

T_{ENDO} . The fibrous β -TPI has a higher degree of crystallinity (0.78). Crystallization at 0°C in amyl acetate followed by annealing in the crystallization liquid at 30°C for a sample with $\bar{M}_n = 2.5 \times 10^5$ gave a crystallinity of 0.63.¹⁵

The formation of α -nuclei under quiescent conditions using material with $\bar{M}_n = 2.5 \times 10^5$ in n-butyl acetate takes place via a non-isothermal crystallization in the β form with these crystals apparently transforming directly or by dissolution and crystallization to give α -nuclei when heated.¹⁴ If the redissolution temperature, T_R , is kept low enough (40 to 45°C), the α nuclei are only partially destroyed and lead to a crystals upon cooling. Heating of these nuclei above 45°C leads to complete destruction of them with subsequent precipitation of the β form upon lowering the temperature below about 20°C, due to its greater nucleation rate.¹⁴ Since the α -modification is the thermodynamically stable form in the presence of a solvent (see Table IX and X), the α -nuclei can not change directly to β -form nuclei in the presence of a solvent. Nuclei of some polymers have been reported to survive in solution to a temperature close to the equilibrium dissolution temperatures of the respective polymers.⁴⁴

In the case of TPI, the α nuclei survives up to temperatures approximately 10°C lower than the respective equilibrium dissolution temperatures. If the nuclei of folded chain crystals differ from the nuclei of extended chain crystals and if there is too much kinetic hindrance in passing from lamellar nuclei to extended chain nuclei then we can expect the temperature up to which the lamellar nuclei are surviving to be the highest temperature to get the lamellar type

of crystals.

Under the conditions used in the present work similar processes to those discussed above for TPI in n-butyl acetate also applies to TPI in n-heptane. It was reported recently¹⁵ that crystallization of TPI with a molecular weight of 2.5×10^5 in n-heptane at 0°C, after dissolution at an elevated temperature, yielded the α -form instead of the β form as reported herein. In that work the concentration was 1% (w/v), the precipitate was in contact with the liquid for one day and drying was carried out at 0°C. It is possible that one or all of these conditions lead to a β to α change; this would be less likely under the conditions of short crystallization period and rapid filtration used in the present work.

The relative stability of α and β forms of TPI was discussed by Flanagan and Rijke¹¹ and a value of 66°C was derived for the temperature at which the free energies of fusion of the two forms are approximately equal. Since the heat of fusion of β -TPI is less than α -TPI (this work and ref. 8 and 11), the β -TPI will be the permanently metastable form with respect to the α -modification if the equilibrium melting point of β -TPI is less than or equal to the equilibrium melting point of α -TPI.⁸ But if the equilibrium melting point of β -TPI is higher than that of the α -TPI then there must be a temperature at which the free energies of fusion of α and β -TPI will be same, and above this temperature, but below the equilibrium melting point, the β -modification will be the stable form of TPI.

The equilibrium melting point of α -TPI has been reported to be lower than that of β -TPI by Flanagan and Rijke,¹¹ but Lovering and

Wooden⁴⁷ and later Davies and Long⁴⁸ reported the opposite. When the melt crystallization of TPI is carried out by slow cooling from an initial sample temperature of 70 - 71°C, the α -form crystallizes exclusively, but cooling from the initial sample temperature above 71°C, the β -form started crystallizing with the α -form (see Fig. 13). Cooper and Vaughan⁹ reported the persistence of nuclei in TPI samples up to 80°C. The persistence of nuclei in the melt of TPI was also reported by Hardin and Yeh.⁸² The slow cooling crystallization method indicates that up to 71°C the α -nuclei in the molten sample of TPI did not convert into β -TPI but did start converting to β -TPI above 71°C and comes to equilibrium at some temperature above 71°C. Since α -nuclei do not show any tendency to convert to β -nuclei below 71°C, 66°C cannot be taken as the temperature where the two forms coexist, as calculated by Flanagan and Rijke.¹¹ However, the conclusion drawn by Flanagan and Rijke,¹¹ that the β -TPI is not a permanently metastable form finds support from this experiment. So, we can conclude that the equilibrium melting point of β -TPI is greater than α -TPI. If we take the equilibrium melting point of α -TPI as 353°K and the heat of fusion value as 10.5 kJ/mole repeat unit, then the equilibrium dissolution temperature of α -TPI in n-butyl acetate can be calculated to be 332°K (see Table IX). Flanagan and Rijke¹¹ determined the equilibrium dissolution temperature of α -TPI in n-butyl acetate by an extrapolation method involving the measurement of dissolution temperature as a function of crystallization temperature and the value is 332°K. This agreement between the calculated and the experimental value suggests that the thermodynamic parameters of melting

used for α -TPI for the calculation of the equilibrium dissolution temperature (T_D^*) in n-butyl acetate, are consistent.

The equilibrium melting point values of α and β -TPI, as given by Flanagan and Rijke¹¹ has been used in the calculations of T_D^* for α and β -TPI in various solvents and for other thermodynamic parameters.

The agreement between T_D , the dissolution temperature determined experimentally, using fibrous stirrer crystallized β -TPI, with T_D^* , the equilibrium value calculated for α -TPI (see Table IX) suggests that the chains are considerably extended and that they transform from $\beta \rightarrow \alpha$ during the dissolution process. It can be noted that T_D experimental for β -TPI in benzene is well below the calculated α -TPI T_D^* . However, Gent⁸³ estimated that the χ values of slightly crosslinked TPI in toluene and benzene to be about the same which suggests that the literature value for χ given for benzene is too large. When it is assumed that T_D for the fibrous β form is actually T_D^* for α -TPI and this is used to calculate χ (Table X), the value for benzene is then within 20% of that for toluene.

The equilibrium dissolution temperatures of β -TPI in n-butyl acetate and heptane have been calculated to be 55 and 47°C respectively, but the highest crystallization temperature attended during the stirrer crystallization of β -TPI from n-butyl acetate and heptane solutions are 48 and 40°C respectively. During the dissolution experimentation with stirrer-crystallized β -TPI ($T_C = 48^\circ\text{C}$ in n-butyl acetate solution) the stirrer crystals must have annealed sufficiently in the presence of diluents⁸⁴ to produce equilibrium crystals of α -TPI.

Mandelkern et al⁸ determined the heats of fusion of α - and β -TPI by an extrapolation method involving measurements of melting points of TPI/methyl oleate and TPI/tetradecane mixtures as a function of concentration of the respective diluents and using the Flory-Huggins Equation.⁵ The Flory-Huggins interaction parameter, χ , of the diluents can also be estimated from this type of study, and Mandelkern et al⁸ reported that the interaction parameter, χ , of both methyl oleate and tetradecane diluents with TPI is approximately zero. The exact cause for the deviations of the reported⁸ values for the methyl oleate and tetradecane/TPI systems from our values are not known. However, a slightly positive χ values for both diluents will lower the reported⁸ ΔH_f° value of α -TPI.

In the calculation of $T_m^*(\alpha)$ using equation 6, ΔH_f° was taken as 10.5 kJ/mol/r.u. One check on the reliability of that number is to obtain dT_m^*/dp using it; the calculated value is found to be within 10% of the measured value.⁶⁰

At the temperature at which the free energy of fusion of the two crystal forms are equal the ratio of the heats of fusion, $\Delta H_f^\circ(\alpha)/\Delta H_f^\circ(\beta)$ should be given by¹¹ $(T_m^*(\beta)-T_m)(T_m^*(\alpha)/T_m^*(\alpha)-T_m)(T_m^*(\beta))$. For $\Delta H_f^\circ(\alpha) = 10.5 \text{ kJ mole}^{-1}$ and $\Delta H_f^\circ(\beta) = 8.0 \text{ kJ mole}^{-1}$, T_m is calculated to be 70°C. This is less than the values of 73-74°C found earlier in this work. However a small error in either ΔH_f° can lead to a large error in the calculated value of T_m .

The fold surface free energies, $\sigma_e(\alpha)$ and $\sigma_e(\beta)$, were calculated earlier⁴⁸ using the same lamellar thickness and melting temperature

results as used in the present work but with different H_f° and T_m^* values. The earlier calculation gave $\sigma_e(\alpha) > \sigma_e(\beta)$ which is the reverse of the current results. In the crystallization process a larger, more unfavorable fold surface free energy could be compensated for by a larger lamellar thickness. For melt crystallization of TPI at temperatures (50-55°C) where data are available for both crystal forms, lamellas in the β form are found to have larger thickness than those in the α form by a factor approximately equal to the ratio of the fold surface free energies calculated in this work. Similarly, when α and β -TPI were crystallized at the same temperature from amyl acetate, the β -TPI was found to be denser¹⁵ than the α -TPI by approximately the same factor as their ratio of fold surface energies. Apparently a favorable surface free energy is not the cause of the appearance of the thermodynamically less stable β -form instead of the α -form at relatively high supercoolings from high temperatures.^{14,48}

The σ_e values of α and β -TPI are nearly 25% to 30% lower than the reported σ_e values of polyethylene.⁷⁴ However, such low values of σ_e have also been reported for isotactic polystyrene,⁷⁴ trans-1,4-polybutadiene^{74,86} (modifications I and II) and cis-1,4-polyisoprene crystals.⁸⁷

The noncrystalline chain traverses present in a stirrer crystallized sample can consist of chain ends, chain folds, interlamellar links and interlamellar defects. The average number of monomer units in a noncrystalline chain traverse, assuming the intralamellar defects to be small in number, was estimated in the preceding section as 36 for the most highly extended fibrous β -TPI. For α -TPI crystals grown

from solution without stirring, this parameter was found^{15,85} to be 6-13. In dilute solution grown crystals using moderate molecular weights ($>10^5$) the component represented by this parameter is composed principally of chain folds. For the fibrous samples extended inter-lamellar links are expected to predominate. The number of monomer units present in the noncrystalline traverse of stirrer-crystallized fibrillar polymer crystals have not been estimated before.

Melting data on a series of flexible linear macromolecules for which equilibrium crystals were available or for which they could be extrapolated are listed with the melting data on Trans-1,4-Polyisoprene (α and β forms) in Table XIV for comparison.

The polymers listed in Table XIV vary in their chemical nature and in the size of the structural repeating unit; hence a wide variation of values for ΔH_f° and ΔS_f° will not be surprising. It can be expected that a major contribution to the entropy of fusion is the increased gain in conformational freedom by the chain segments on melting. ΔS_f° would then be expected to increase as the number of chain atoms in a repeating unit increases. A more rational basis of comparison between different unit might then be achieved by dividing the observed ΔS_f° by the number of single bonds in the repeating unit. However, it must be realized that besides the conformational freedom gained on melting there can be other contributions to the entropy of fusion. In particular, one must give consideration to the contribution due to the volume change that occurs on melting. For ΔH_f° , the major contribution is expected to come from the loss of interaction on expansion to the liquid state. So a more rational basis

TABLE XIV
 Thermodynamic Parameters Characterizing the
 Fusion of Flexible Linear Polymer⁵⁰

No.	Polymer	T_m^*	$\Delta H_f^{\circ a}$	$\Delta S_f^{\circ a}$	Cohesive Energy Density kJ/mole
		K	kJ/mole	J/K/mole	
1.	Polyethylene	415	4.1(2)	9.9(2)	4.2
2.	Polytetrafluoroethylene	600	3.42(2)	5.7(2)	3.35
3.	Isotactic Polypropylene (α)	456	3.7(3)	11.9(2)	4.7
4.	Isotactic Polybutene-1 (modification I)	414	1.8(4)	8.5(2)	4.6
5.	Isotactic Polypentene-1	403	1.3(5)	7.8(2)	4.5
6.	Poly-4-methyl-1-pentene	523	1.7(6)	9.5(2)	4.7
7.	Isotactic Polystyrene	516	1.3(8)	9.7(2)	4.7
8.	Cis 1,4-Polybutadiene	310	0.9(5)	4.8(3)	4.2
9.	Trans 1,4-Polybutadiene (Ref. 50,74)	415	1.0 ₅ (4)	3.4(3)	4.2
10.	Cis 1,4-Polyisoprene	310	0.9(5)	4.8 (3)	3.9
11.	Trans 1,4-Polyisoprene (Ref. 93) (α)	353	2.1(5)	9.9(3)	3.9
12.	Trans 1,4-Polyisoprene (Ref. 93) (β)	356	1.6(5)	7.5(3)	3.9

Table XIV Continued

No.	Polymer	T_m^*	$\Delta H_f^{\circ a}$	$\Delta S_f^{\circ a}$	Cohesive Energy Density
		K	kJ/mole	J/K/mole	kJ/mole
13.	Trans 1,4-Polychloroprene (Ref. 85)	378	1.6(5)	7.0(3)	-
14.	Polyoxymethylene	457	4.9(2)	10.7(2)	5.2
15.	Polyethylene oxide	342	2.9(3)	8.4(3)	4.9
16.	Polyethylene terephthalate	553	2.2(12)	9.6(5)	5.0
17.	Nylon 6, (α)	533	3.7(7)	8.1(6)	11.7
18.	Nylon 8, (γ)	491	2.0(9)	4.5(8)	10.0
19.	Nylon 6.6 (α)	553	4.8(14)	10.2(12)	11.7

^a The number of units in the repeating unit is given in parenthesis. Flexible chain units for ΔS_f° and total interacting groups for ΔH_f° .

of comparison of ΔH_f° between different polymeric units might be achieved by dividing the observed ΔH_f° by the number of interacting groups present in the repeating unit.

In Table XIV, column 3 gives the melting temperature in degrees Kelvin; column 4 gives the heat of fusion per mole of interacting groups, which is the total number of interacting groups per repeating unit, given in parentheses. It involves counting all large atoms,

disregarding only H, and counting CO- as one unit. Column 4 gives the entropy of fusion per rigid backbone chain group (CR_1R_2- , $O-$, $CR=CH-$, $COO-$, C_6H_4- , and $CONH-$). The number of rigid chain groups per repeating unit is given in parenthesis. Column 6 contains the cohesive energy density per mole of amorphous, interacting groups (as in column 4).

The entropy of fusion of the majority of macromolecules is between 8 to 10 JK/mole of rigid backbone chain groups. There are six exceptional macromolecules (2,9,10,12,13 and 16) with frequently much smaller entropies of fusion. A check of the crystal structure or melting behavior of these macromolecules suggests that these crystals have high temperature crystal forms that contain already increased disorder.

Turning now to the macromolecules for which the chains are practically in a fixed, perfectly ordered conformation before melting, one expects a large portion of the entropy of fusion to be purely conformational in origin. Comparing the experimental data with calculated entropies of fusion, one finds typically 65 - 85% for the contribution of conformational entropy to the total entropy of fusion. In the cases of trans-1,4-polyisoprene (α and β) and cis-1,4-polyisoprene,^{8,89,93} a large portion (> 50%) of entropy of fusion originated from the entropy change due to volume expansion of fusion. The low temperature modifications of trans-1,4-polybutadiene, which has similar chain structure as that of trans 1,4-polyisoprene (β -form) in the unit cell⁹⁰ shows considerable gain in entropy during the solid-solid transition to the high temperature modification probably

due to the volume expansion that occurs during the transition.^{16,91} The almost two-fold difference in the entropies of fusion between cis-1,4-polyisoprene and trans-1,4-polyisoprene (α -form) may be related to the greater relative extension in space of cis-1,4-polyisoprene as compared to the trans-1,4-polyisoprene in the amorphous state.^{8,92,93}

Among the macromolecules with a high entropy of fusion further trends can be seen on inspection of Table XIV. Macromolecules with phenylene groups within the backbone seem to have a somewhat increased entropy over similar molecules that contain CH_2 - groups. When CH_2 - and other functional groups such as O-, COO-, alternate one also has higher entropies of fusion. Much of this difference may be connected with the change in crystal and liquid structure relative to an increased non-polar CH_2 - environment. At present it is not possible to decide whether these trends are based on conformational or nonconformational effects.

The average heat of fusion of the polymers listed in Table XIV is 2.4 kJ mole^{-1} . All macromolecules with exceptionally small entropies of fusion show also heat of fusion substantially lower than the average value of 2.4 kJ mole^{-1} . Examples are cis-1,4-polyisoprene, trans-1,4-polychloroprene and the high temperature form of trans-1,4-polybutadiene. The polyamides, (No. 17 and 19) have a 1-2 kJ mole^{-1} higher heat of fusion than the average; which goes parallel with their much higher cohesive energy density. The macromolecules with larger side chain (4-7) have also a lower heat of fusion than the average when calculated per total of single interacting group. Finally, polyethylene, polypropylene (isotactic), polytetrafluoroethylene and polyoxymethylene have a 1-2 kJ mole^{-1} higher heat of

fusion.

Although the cohesive energy densities and changes in packing fraction can explain some of the changes in heat of fusion with chemical structure, they are not sufficient. One must add the intramolecular contributions to the heat of fusion that results from the change to some high-energy conformations on fusion. A particularly clear example is polyethylene, where in the crystal, only the low-energy trans conformation is found. In the melt, however, each carbon-carbon bond may also be in one of the two gauche conformations that are higher in energy by 2 kJ mole^{-1} . At the melting temperature, the high temperature limit of equal distribution among the three rotational isomers is not quite reached, but even on equal distribution among trans and gauche conformations, the intramolecular heat of fusion would be 1.0 kJ mole^{-1} , or about 25% of the total heat of fusion.

Combining now all the conclusions on entropy of fusion, cohesive energy density, and heat of fusion, one can make some general statements about the melting temperatures of flexible linear macromolecules:

The high melting temperature of polyethylene(1) relative to cis-polybutadiene(8) does not rest with a higher conformational entropy of fusion but rather with the higher heat of fusion of polyethylene, a good part of which must result from intramolecular contributions and the larger volume change on fusion. The trans-polydienes, particularly in their high-temperature form (9) with an all trans conformation in the crystal, have a melting temperature close

to that for polyethylene, as one would expect.

Particularly high-melting flexible chain polymers are polytetrafluoroethylene(2), isotactic poly-4-methyl-1-pentene(6), and isotactic polystyrene(7). The polytetrafluoroethylene melting temperature is elevated due to the low value of entropy of fusion. The other two macromolecules have, in contrast, a high melting temperature because of a high molar heat of fusion.

Polyoxymethylene(14) does not have, as was frequently suggested, a low entropy of fusion; instead its relatively high-equilibrium melting temperature must be connected, as in polyethylene, with an exceptionally high heat of fusion. Only a part of the increased heat of fusion can be accounted for by the higher cohesive energy contribution of the oxide group. Some of the increase must also come from intramolecular sources. The higher analog (15) drops to level much more in line with "normal" macromolecules.

The polyester(16) has 12 interacting groups and 5 rigid backbone groups. So, ΔH_f° per mole of repeat unit = (2.2×12) kJ and $\Delta S_f^\circ = (9.6 \times 5)$ J/K (see Table XIV). The large difference between the number of rigid backbone chain groups and the total number of interacting groups in the polyester(16) increases the value of $\Delta H_f^\circ/\Delta S_f^\circ$ and hence the melting point.

The polyamides(17-19) owe their high melting temperatures to their high heats of fusion. The amide group has a cohesive energy density per backbone chain atom 7.3 times that of CH_2 -. This is in contrast to the ester and oxide groups, which are only 1.6 and 1.5 times higher in cohesive energy density per chain atom than CH_2 -.

CONCLUSIONS

Measurements of both density and melting endotherm for stirrer crystallized trans-1,4 polyisoprene show a clear change from lamellar to fibrous morphology which also corresponds with a change of crystal form from α to β .

Further evidence is given to show that the diluent-induced β to α transformation is of considerable importance in determining the polymorphic composition during TPI crystallization from solution.

Results of the present work involving measurement or calculation of various thermodynamic parameters are consistent with the β -form having the higher equilibrium melting point as suggested earlier by Flanagan and Rijke. However the enthalpy of fusion measured by those workers believed to be for the β -form is actually that for the α -form due to β to α transformation in the liquid present.

Analysis of experimental data allows for the establishment of the equilibrium dissolution temperatures of α - and β -TPI in various liquids and for the calculation of the Flory-Huggins interaction parameter.

Calculation of fold surface free energy led to a lower value for the α -form (42 ± 1 ergs cm^{-2}) than for the β -form (53 ± 1 ergs cm^{-2}) a reversal of earlier results.

A method for estimating the number of monomer units per average non-crystalline chain traverse for fibrous β -TPI was given.

SUGGESTIONS FOR FUTURE WORK

1. The highest crystallization temperature, at which stirrer crystallization can be done from solution of TPI in n-butyl acetate or heptane, is found to be lower than the equilibrium dissolution temperatures of α - and β -TPI in those solvents. With the increase of crystallization temperatures the length of the fibrous crystals in the "shish" (central core) increases and results in high fiber strength.⁴³ Recently Pennings et al.,⁴³ have developed the "Surface-growth technique" by which crystallization can be conducted from solution of a polymer up to the equilibrium dissolution temperature of that polymer. It would be of interest to see the type of modification appearing at higher crystallization temperatures than those attainable by the stirrer crystallization technique, and whether it is possible to make α -TPI by crystallizing from solution of TPI at crystallization temperatures above the equilibrium dissolution temperature for β -TPI. A study of the melting behavior of α -TPI fibrous crystals thus prepared, calculation of the percentage crystallinity from density measurement and the number of monomers interconnecting between the fibrous crystals would also be of interest.
2. A different route for growing extended chain crystals of a polymer is by crystallization during polymerization. By this method polyethylene oxide crystals have been grown in the extended state.⁴⁵ Polychloroprene, which has a crystal structure similar to β -TPI, has also been grown in the extended state by polymerizing chloroprene near its glass transition temperature by β -radiation.⁸⁵ It may be

possible to crystallize TPI in the extended state by this method and then to study its melting behavior, polymorphic composition and percentage crystallinity. It will also be of interest to see, whether the morphology of the resulting crystals are shish-kebob type or of only fibrous type.

3. Lovering et al.¹⁰ reported that only β to α -conversion can be conducted by fusing β -TPI first. No solid-solid transition has not been found to occur. But in the presence of diluents β -TPI converts to α -TPI without apparently any disintegration of the samples and without any loss of the opacity of the β -TPI crystals^{7,14} (including the stirrer crystallized samples). If the diluents can penetrate the β -TPI lattice, then before the damages of the overall structure of β -crystal lattices occurred, α -form of crystal lattices must originate. The detail of the mechanism of the diluent induced transformation of β -TPI to α -TPI has not been elucidated to date. By using calorimetric methods and taking wide angle x-ray diffraction photographs of the swelled samples of β -TPI with increasing time, the mechanism of the transformation can be known. Since the amount of heat required for the β -solid to α -solid transition in the presence of a diluent is lower than the heat of dissolution of β -TPI crystals, it should be possible to follow the process of transformation calorimetrically.

REFERENCES

1. D. Fisher, Proc. Phys. Soc. London, B66, 7 (1953).
2. Y. Takahashi, T. Sato, T. Tadokoro and Y. Tanaka, J. Polym. Sci. Polymer Phys. Ed., 11, 233 (1973).
3. C. W. Bunn, Proc. Roy. Soc. London, Ser. A. A180, 40 (1942).
4. H. Hopff and G. von Susich, Kautschuk, 6, 234 (1930).
5. E. A. Hauser and G. von Susich, Kautschuk, 7, 120, 125, 145 (1931).
6. J. N. Dean, Trans. Inst. Rubber Ind., 8, 25 (1932).
7. H. M. Leeper and W. Schlesinger, J. Polym. Sci., 11, 307 (1953).
8. L. Mandelkern, F. A. Quinn, Jr., and D. E. Roberts, J. Am. Chem. Soc. 78, 926 (1956).
9. W. Cooper and G. Vaughan, Polymer, 4, 329 (1963).
10. E. G. Lovering and D. C. Wooden, J. Polym. Sci. A-2, 7, 1639 (1969).
11. R. D. Flanagan and A. M. Rijke, J. Polym. Sci. A-2, 10, 1207 (1972).
12. A. Keller and E. Martuscelli, Makromol. Chem., 151, 189 (1972).
13. H. M. Rootare and J. M. Powers, J. Dent, Res., 36, 1453 (1977).
14. K. Anandakumaran, C. C. Kuo, S. Mukherji and A. E. Woodward, J. Polym. Sci. Polym. Phys. Ed., 20, 1669 (1982).
15. C. C. Kuo and A. E. Woodward, Macromolecules., 17, 1034 (1984).
16. F. Danusso, Polymer, 8, 281 (1967).
17. P. J. Flory, "Principles of Polymer Chemistry", Cornell Univ. Press, Ithaca, N.Y. 1953 p. 563.
18. J. F. Jackson, L. Mandelkern and O. C. Long, Macromolecules, 1, 218 (1968).
19. K. H. Storks, J. Amer. Chem. Soc., 60, 1753 (1938).
20. P. H. Till, J. Polym. Sci., 24, 301, (1957).
21. A. Keller, Phil. Mag., 8, 1171 (1957).

22. E. W. Fischer, Z. Naturforsch, 12a, 753 (1957).
23. W. Schlesinger and H. M. Leeper, J. Polym. Sci., 11, 203 (1953).
24. A. Keller, Makromol Chem., 34, 1 (1959).
25. A. Keller, Polymer, 3, 393 (1962).
26. P. Geil, "Polymer Single Crystals", Wiley Interscience, New York, (1963).
27. P. J. Flory, J. Amer. Chem. Soc., 84, 2857 (1962).
28. L. Mandelkern, Accounts Chem. Res., 9, 81 (1976).
29. S. Tseng and A. E. Woodward, Macromolecules, 15, 343 (1982).
30. B. Wunderlich, J. Chem. Phys., 29, 1401 (1958).
31. J. D. Hoffman and J. I. Lauritzen, Jr., J. Res. Natl. Bur. Stand. 65A, (1961).
32. J. D. Hoffman, G. T. Davis and J. I. Lauritzen, Jr., in "Treatise on Solid State Chemistry" (Ed. N. B. Hannay), Plenum Press, New York, 1976, Vol. 3 Ch. 7.
33. A. J. Pennings and A. M. Kiel. Kolloid Z-Z. Polym., 205, 160 (1965).
34. A. J. Pennings, J. Polym. Sci., Part C, 16, 1799 (1967).
35. A. J. Pennings, J. J. A. A. van der Mark, and H. C. Booij, Kolloid Z-Z. Polym., 236 99 (1970).
36. A. J. Pennings, J. A. van der Mark and A. M. Kiel, *ibid*, 237, 336 (1971).
37. A. J. Pennings, Makromol. Chem., Suppl., 2, 99 (1979).
38. A. M. Rijke and L. Mandelkern, J. Polym. Sci., A-2, 8, 225 (1970).
39. E. Kobayashi, S. Okamura and R. Signer, J. Appl. Polym. Sci., 12, 1661 (1968).
40. A. Wikjord and R. St. John Manley, J. Macromol. Sci. (Phys.), B4, 397 (1970).
41. B. C. Edwards and P. J. Phillips, J. Mater. Sci., 9, 1382 (1974).
42. M. Kyotani, J. Macromol. Sci.(Phys.), B21, 275 (1982).

43. A. Keller and P. J. Barham, *Plastics and Rubber International*, 6, 19 (1980).
44. D. J. Blundell, A. Keller and A. J. Kovacs, *J. Polym. Sci., Polym. Lett. Ed.*, 4, 481 (1966).
45. B. Wunderlich, "Macromolecular Physics", Vol. 2, Academic Press, New York, (1976).
47. E. G. Lovering and D. C. Wooden, *J. Polym. Sci. A-2*, 9, 175 (1971).
48. C. K. L. Davies and O. E. Long, *J. Mater. Sci.*, 14, 2529 (1979).
49. C. Devoy and L. Mandelkern, *J. Polym. Sci. A-2*, 7, 1883 (1969).
50. B. Wunderlich, "Macromolecular Physics", Vol. 3, Academic Press, New York, (1980), p. 39-41, 91-96.
51. H. Hendus and K. H. Illers, *Kunststoffe* 52, 69 (1967).
52. E. W. Fischer and G. Hinrichsen, *Kolloid Z.-Z. Polym.* 247, 858 (1971).
53. S. Tseng, W. Herman, A. E. Woodward and B. A. Newman, *Macromolecules*, 15, 338 (1982).
54. L. Mandelkern, "Crystallization of Polymers", McGraw-Hill Book Co., New York (1964), Chap. 5.
55. R. A. Oriani, *J. Chem. Phys.*, 19, 93 (1953).
56. J. C. Slater, "Introduction to Chemical Physics", McGraw-Hill Book Co., New York (1939).
57. A. E. Tonelli, *J. Chem. Phys.*, 52, 4749 (1970).
58. P. J. Flory, "Statistical Mechanics of Chain Molecules", Interscience, New York (1968).
59. P. J. Flory and R. L. Jernigan, *J. Chem. Phys.*, 42, 3509 (1965).
60. M. Naoki and T. Tomomatsu, *Macromolecules*, 13, 322, (1980).
61. J. E. Mark, *J. Amer. Chem. Soc.*, 88, 4354 (1966).
62. Y. Abe and P. J. Flory; *Macromolecules*, 4, 230 (1971).
63. G. Schuur, "Some Aspects of the Crystallization of High Polymers", Rubber-Stichting, Delft, Netherlands, (1955).

64. E. Fischer and J. F. Henderson, *J. Polym. Sci. A-2*, 5, 377 (1967).
65. G. Allegra and M. Bruzzone, *Macromolecules*, 16, 1167 (1983).
66. R. A. Swalin, "Thermodynamics of Solids", John Wiley and Sons, Inc., New York (1962) pages 74-78.
67. P. L. McGeer and H. C. Duus, *J. Chem. Phys.*, 20, 1813 (1952).
68. H. W. Starkweather, Jr., P. Zoller and G. A. Jones, *J. Polym. Sci. Polym. Phys. Ed.*, 21, 295 (1983).
69. T. Kijima, M. Imamura and N. Kusumoto, *Polymer*, 17, 249 (1976).
70. C. Nakafuku, *Polymer*, 22, 1673 (1981).
71. H. W. Starkweather, Jr., P. Zoller, G. A. Jones and A. J. Vega, *J. Polym. Sci. Polym. Phys. Ed.*, 20, 751 (1982).
72. G. Bautz, U. Leute, W. Dollhopf and P. C. Haegeler, *Colloid and Polym. Sci.*, 259, 714 (1981).
73. S. Mukherji, unpublished results.
74. A. Marchetti and F. Martuscelli, *J. Polym. Sci. Polym. Phys. Ed.*, 14, 151 (1976).
75. M. W. Duch and D. M. Grant, *Macromolecules*, 3, 165 (1970).
76. M. J. Fernandez-Berridi, F. J. Ansorena, J. J. Irwin and G. M. Guzman, *Macromolecules*, 13, 190 (1980).
77. M. L. Huggins, *Ann. N. Y. Acad. Sci.*, 44, 431 (1943).
78. C. Nakafuku and T. Miyaki, 24, 141 (1983).
79. C. D. Armeniades and J. F. Baer, *J. Macromol. Sci. (Phys.)*, B1, 309 (1967).
80. E. Baer and J. L. Kardos, *J. Polym. Sci. Part A*, 3, 2827 (1965).
81. U. Laute, W. Dollhopf and E. Liska, *Colloid. Polym. Sci.*, 256, 914 (1978).
82. I. R. Hardin and G. S. Yeh, *J. Macromol. Sci. (Phys.)*, B7, 393 (1973).
83. A. N. Gent, *J. Polym. Sci. A-2*, 4, 447 (1966).
84. J. H. Magill, *J. Polym. Sci. Polym. Lett. Ed.*, 20, 1 (1982).

85. K. Anandakumaran, W. Herman and A. E. Woodward, *Macromolecules* 16, 563 (1983).
86. J. Finter and G. Wegner, *Makromol. Chem.*, 182, 1859 (1981).
87. E. N. Dalal and P. J. Philips, *Macromolecules*, 17, 248 (1984).
88. R. R. Garrett, C. A. Hargreaves and D. N. Robinson, *J. Macromol. Sci.(Chem.)*, A4, 1679 (1970).
89. L. Mandelkern, *Chem. Rev.*, 56, 903 (1956).
90. G. Natta and P. Corradini, *Nuovo Cim. Suppl.*, 15, 9 (1960).
91. G. Moraglio, G. Polizzotti and F. Danusso, *Eur. Polym. J.*, 1, 183 (1965).
92. H. L. Wagner and P. J. Flory, *J. Amer. Chem. Soc.*, 74, 195 (1952).
93. S. Mukherji and A. E. Woodward, *J. Polym. Sci. Polym. Phys. Ed.*, 22, 793 (1984).